# Analogies in Classical Physics

Daniele Battesimo Provenzano\*

February 8, 2025

#### Abstract

In this lecture, we will examine in detail several analogies between phenomena belonging to different branches of Classical Physics which, perhaps surprisingly, are governed by the same mathematical models. Did you know that light rays can bend so as to form closed orbits, and that Snell's law also governs the propagation of seismic waves through earth's crust? Or that the velocity distribution of a river flowing around a bridge pier is mathematically identical to the electric field produced by two charges placed very far from a disk with null permittivity? And did you know that the motion of hatchling turtles on a beach, while escaping from crabs, provides a direct analogy for how visibility is reduced on a foggy day? By the end of this lecture, you certainly will  $\odot$ .

 $<sup>{}^*</sup> daniele. provenzano@sns. it \ or \ daniele. battesimo. provenzano@gmail.com$ 

## — CONTENTS

1	Evanescence in Every Flavor	3
2	Mechanical and Circuit Resonance 2.1 Damped Harmonic Oscillator	8
	2.1 Damped Harmonic Oscillator	
3	Snell's Law in Every Flavor	13
	3.1 Derivation of Snell's Law	15
	3.2 Inferior and Superior Mirages	17
4	Orbits in Optics and in Radial Force Fields	18
5	Orbit Decay	21
6	Analogy Between Electrostatics and Fluid Dynamics	23
	6.1 Electric Field and Velocity Field	23
	6.2 Method of Images	24
	6.3 Examples of Fields and Flows in 2D	
	6.4 Examples of Fields and Flows in 3D	
	6.5 Force on Conductors and Obstacles	

## sez. 1 — EVANESCENCE IN EVERY FLAVOR

Attenuation and evanescence both refer to the spatial decay of physical quantities. In this section, we will see how evanescence underlies phenomena that, at first glance, appear very different from one another.

**Example 1.1** (Poor Turtles). Sea turtles lay their eggs on beaches. The nests must be far enough from the water to avoid being swept away by waves, so hatchlings must cross a stretch of sand full of predators before reaching the sea. Consider a rectangular beach patch with sides  $L_x$  and  $L_y$ . Assume that  $N_0$  turtles hatch at the same time at a distance  $L_x$  from the water and that nests are uniformly distributed along the side of length  $L_y$ . When they hatch, turtles head toward the water at constant speed v and can be considered point-like. Unfortunately, the beach has  $N_C$  crabs, uniformly distributed and stationary, which eat all turtles within a distance  $r_C$  of them.

- 1. How many turtles are still alive at a distance x from the nests?
- 2. How would the answer change if the crabs had finite reaction time  $t_r$ ?

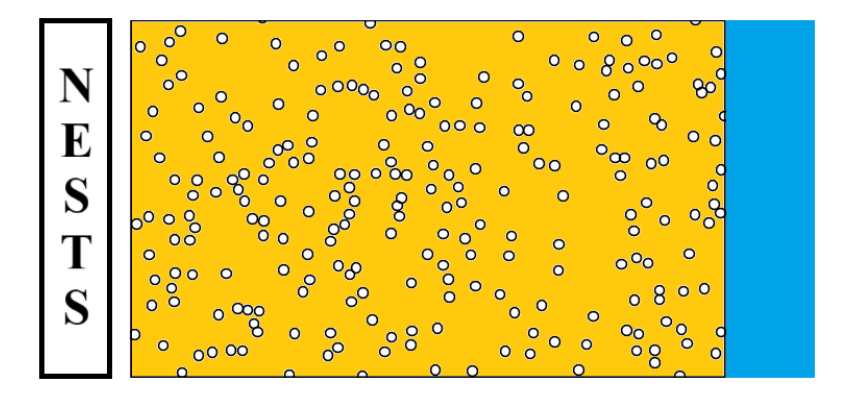


Figure 1: Schematic of the beach patch through which the turtles move. White circles represent the visual fields of the crabs.

Let us begin by stressing that the following solution is valid only in the limiting configuration where the number of crabs is very large and  $r_C$  is small, as shown in Fig. 2.

1. Let us first notice that the solution does not depend at all on the turtles' speed. Indeed, since the crabs have zero reaction time, a turtle is captured instantly as soon as it enters their action radius.

Let us then consider a strip of beach at distance x from the nests, of length  $L_y$  and infinitesimal thickness dx. The turtles that die in this region are

$$dn(x) = -n(x) \frac{2 r_C N_C}{L_x L_y} dx.$$

Let us justify this expression in detail. The density of crabs on the beach is

$$\eta_g = \frac{N_C}{L_x L_y},$$

so in the strip there are

$$\eta_g L_y \mathrm{d}x = \frac{N_C}{L_x} \, \mathrm{d}x$$

crabs.

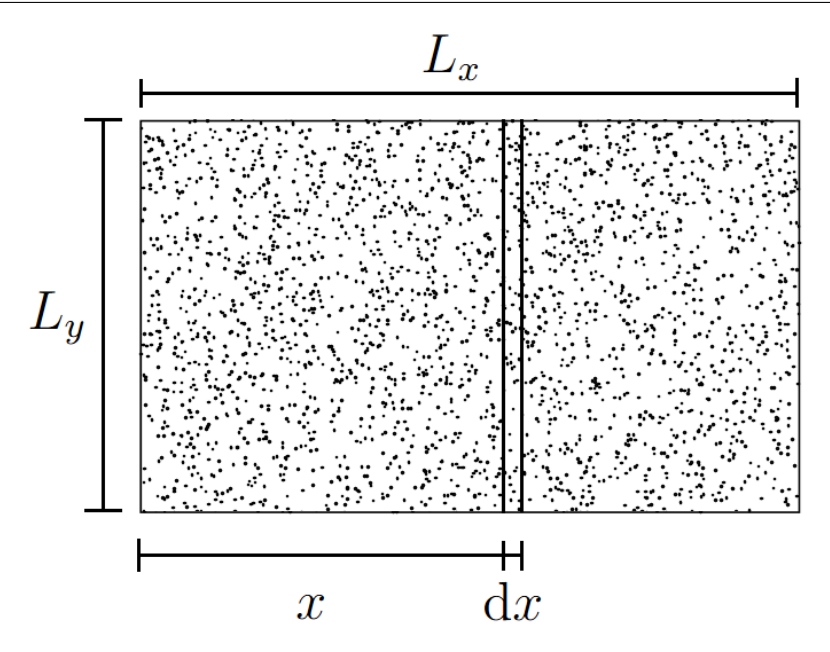


Figure 2: Schematic of the beach patch along which the turtles move. Black dots represent the visual fields of the crabs.

Because the crabs are homogeneously distributed, the fraction of turtles that die equals the fraction of space covered by their visual fields along  $L_y$ . Each crab covers a length  $2r_C$ , therefore the fraction covered is  $(2r_C/L_y)$ . Translating into formulas, we obtain

$$\frac{\mathrm{d}n(x)}{n(x)} = -\left(\frac{2r_C}{L_y}\right)\left(\frac{N_C}{L_x}\,\mathrm{d}x\right).$$

The minus sign reminds us that dn(x) is negative because turtles die. The first factor  $2r_C/L_y$  is the fraction of length covered by a single crab, while the second factor is the number of crabs in the strip. Solving, we find

$$n(x) = N_0 e^{-\frac{2r_C N_C}{L_x L_y} x}.$$

Thus, the number of turtles that manage to reach the sea is

$$n(x = L_x) = N_0 e^{-\frac{2r_C N_C}{L_y}}.$$

2. Let us now analyze the effect of finite reaction time  $t_r$ . In this case, the effective coverage length of each crab is smaller than  $2r_C$ , since depending on its position a turtle can escape the danger zone before the crab notices it. The faster the turtle, the smaller the effective length of danger.

A simple geometric reasoning, applied to the circle of radius  $r_C$  centered on a crab, yields the effective covered length:

$$2\sqrt{r_C^2 - \frac{1}{4}v^2t_r^2}.$$

This reduces to  $2r_C$  in the zero-reaction-time limit. The expression ceases to hold when  $vt_r > 2r_C$ , i.e., when the distance traveled by a turtle during the reaction time exceeds the circle's diameter. In this case, no turtle dies, because no crab notices them — they are too fast!

Restricting to  $vt_r \leq 2r_C$ , the number of surviving turtles at distance x is

$$n(x) = N_0 e^{-\frac{N_C \sqrt{4r_C^2 - v^2 t_r^2}}{L_x L_y}} x.$$

**Example 1.2** (Visibility in Fog). We are on a highway on a foggy day; visibility is 50 m. What is the density of water droplets dispersed in air? Derive an analytic expression and provide a numerical estimate using reasonable values for the quantities involved in the solution.

Let us view this problem as the three-dimensional analogue of the previous one. The effective cross-section of a fog droplet is

$$S = \pi R^2$$
.

In a slab of thickness dx at depth x, the number of light rays is diminished by

$$dn(x) = -n(x) \pi R^2 \eta dx,$$

where n(x) is the number of rays not yet scattered and  $\eta$  is the density of fog droplets. Solving this differential equation, we find

$$n(x) = n_0 e^{-\pi R^2 \eta x},$$

where  $n_0$  is the number of emitted rays.

We can define visibility as the distance over which the number of unperturbed rays is reduced by a factor e. Then

$$d = \frac{1}{\pi R^2 \eta} \qquad \Longrightarrow \qquad \eta = \frac{1}{50 \, \text{m} \cdot \pi R^2}.$$

The radius of fog droplets varies, but for continental fog it is typically a few microns. It follows that

$$\eta \approx 10^8 - 10^9 \, droplets/m^3$$
.

**Example 1.3** (Photonic Pinball). Model an interstellar cloud as a homogeneous slab, thin compared to its other dimensions, composed of interstellar dust grains approximated as small spheres of radius R. A flux  $F_I$  of photons (per unit time and area), from a distant star, impinges on the cloud perpendicular to one of its large faces. Inside the cloud photons are not absorbed by the grains but bounce off them like pinballs, maintaining their frequency. Some photons pass through the cloud, others are reflected backward. If the grain density in the cloud is  $\eta$  and the cloud thickness is L, how many photons pass through the cloud in steady state?

At first, one might be tempted to expect an exponential solution as in the previous examples. But let us note the crucial difference: photons are not absorbed, but rather reflected. In Example 1.1, turtles disappear when eaten by crabs, just as in Example 1.2 photons were assumed absorbed by fog particles.

Does this assumption make sense? Let us reflect: although photons in fog are not literally absorbed, our model still works because photons deviated by scattering no longer carry correct directional information. Only photons that preserve their straight path contribute to good visibility.

Here, however, we must explicitly account for reflection. Let us notice that the number of transmitted photons will be greater than in the absorption case, since a photon scattered once may later be scattered back forward and transmitted. Each photon therefore undergoes a random walk, as shown schematically in Fig. 3.

Given the cloud's geometry, let us restrict to the one-dimensional case, with x representing depth. The random walk is described by Fick's law and the diffusion equation:

$$\mathcal{F}(x,t) = -D \frac{\partial n(x,t)}{\partial x}, \qquad \frac{\partial n(x,t)}{\partial t} = D \frac{\partial^2 n(x,t)}{\partial x^2},$$

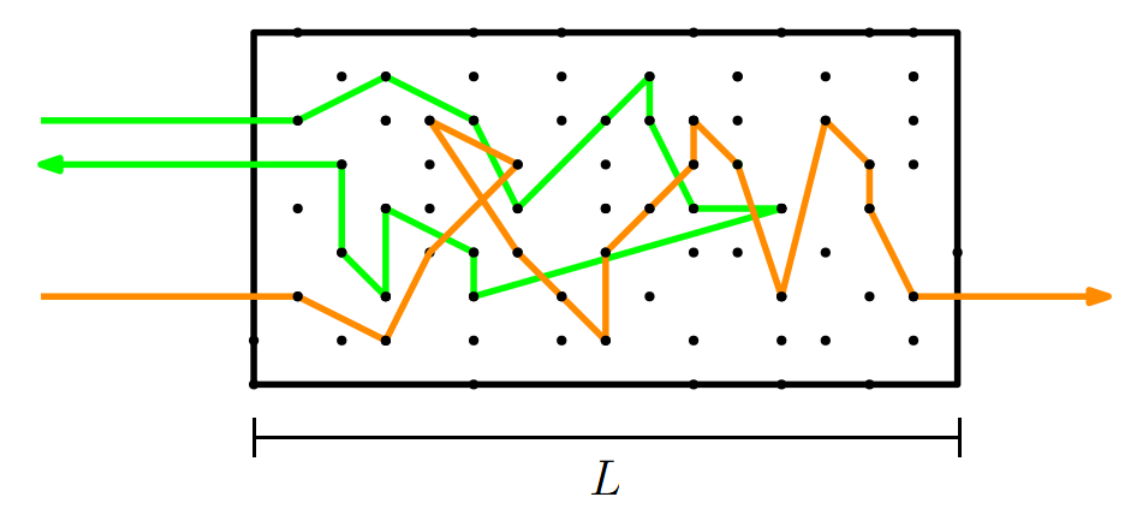


Figure 3: Random walk of two photons, one reflected and one transmitted.

where n(x,t) is the photon density at depth x and time t,  $\mathcal{F}(x,t)$  is the net photon flux, and D is the diffusion coefficient.

The mean free path of photons in a medium of density  $\eta$  and particle radius R is

$$\lambda = \frac{1}{\pi R^2 \eta}.$$

Since the photon speed is c, we obtain

$$D = \frac{c}{\pi R^2 \eta}.$$

We are asked to study a steady-state situation, i.e., equilibrium. Let us therefore remove the time dependence:

$$\mathcal{F}(x) = -D\frac{\mathrm{d}n(x)}{\mathrm{d}x}, \qquad \frac{\mathrm{d}^2n(x)}{\mathrm{d}x^2} = 0.$$

The solution of the second equation is linear:

$$n(x) = Ax + B$$
.

with constants A, B determined by boundary conditions.

• At x = L, for transmitted photons:

$$n(L) = n_T$$
.

• At x = 0, the density includes incident and reflected photons:

$$n(0) = n_I + n_R,$$

with

$$n_I = \frac{F_I}{c}, \quad n_R = \frac{F_R}{c}, \quad n_T = \frac{F_T}{c}.$$

Let us verify these relations. Consider incident photons: in a time  $\Delta t$ , N photons move a distance  $c\Delta t$ , occupying volume  $\Delta V = Sc\Delta t$ , where S is the cross-sectional area of the flux tube. The photon flux is  $F_I = N/(S\Delta t)$ . The density is  $n_I = N/\Delta V = F_I/c$ . Similar reasoning applies to  $n_R$  and  $n_T$ .

Also note: the net photon flux at x = 0 is  $\mathcal{F}(0) = F_I - F_R$ . Why the minus sign here, whereas for density we added? Because fluxes are directed quantities (vectors), while density is scalar.<sup>1</sup> Imposing the conditions and using conservation of total flux,

$$F_I = F_R + F_T \implies n_I = n_R + n_T$$

we obtain

$$n(x) = \frac{2(n_T - n_I)}{L} x + 2n_I - n_T.$$

This decreases with x, as expected. The photon flux is

$$\mathcal{F}(x) = -D \frac{\mathrm{d}n(x)}{\mathrm{d}x} = \frac{2D}{L}(n_I - n_T),$$

which is uniform throughout the cloud, consistent with the steady-state assumption.

At depth x = L we have

$$\mathcal{F}(L) = F_T = \frac{2D}{L}(n_I - n_T).$$

Substituting D, we find

$$n_T = \frac{2n_I}{2 + \pi R^2 \eta L}.$$

Thus, for finite L, this is always larger than

$$n_T = n_I e^{-\pi R^2 \eta L}$$

the exponential absorption case. The comparison is shown in Fig. 4.

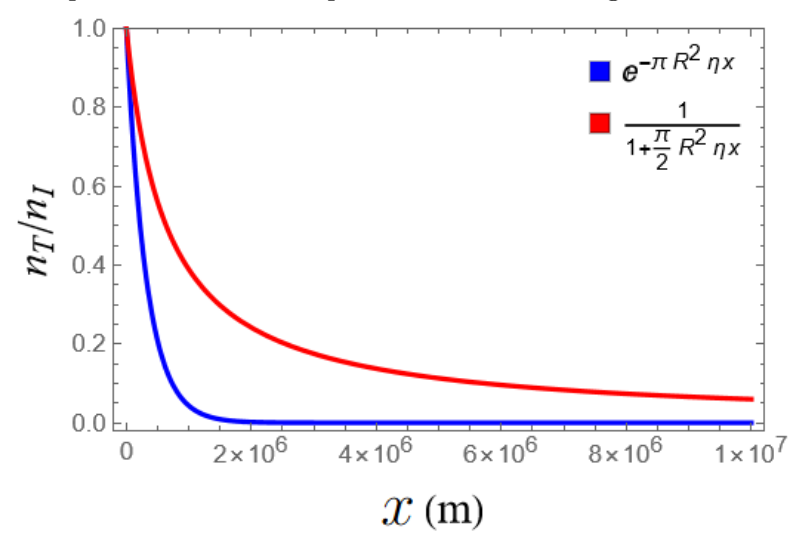


Figure 4: Comparison of the two functions describing light-intensity attenuation: exponential decay with absorption (as in fog) and diffusion with scattering (as in the interstellar cloud). Parameters:  $R = 10^{-6}$  m and  $\eta = 10^{6}$  m<sup>-3</sup>.

Example 1.4 (Evanescence of Electromagnetic Plane Waves). Consider a monochromatic electromagnetic plane wave propagating along  $\hat{x}$ , with electric field

$$\vec{E}(x,t) = \vec{E}_0 e^{i(kx-\omega t)}.$$

where  $\vec{E}_0$  is a constant vector (the amplitude), k is the wavenumber, and  $\omega$  the frequency. In physics, any wave has an associated dispersion relation linking k and  $\omega$ . For plane electromagnetic

<sup>&</sup>lt;sup>1</sup>Even if it is not evident in one dimension, fluxes are vectors. In two or three dimensions, this would be obvious; here we omit arrows for simplicity.

waves propagating in an isotropic medium with permittivity  $\varepsilon_0\varepsilon$  and permeability  $\mu_0\mu$ , derive the dispersion relation and discuss what happens when  $\varepsilon\mu$  is negative or complex.

Let us recall that k and  $\omega$  cannot be chosen independently, but are linked by a dispersion relation. In an isotropic medium with relative permittivity  $\varepsilon$  and permeability  $\mu$ , the wave equation is

$$\frac{\partial^2 \vec{E}}{\partial x^2} = \varepsilon_0 \varepsilon \mu_0 \mu \frac{\partial^2 \vec{E}}{\partial t^2} = \frac{\varepsilon \mu}{c^2} \frac{\partial^2 \vec{E}}{\partial t^2},$$

where c is the speed of light in vacuum.

Substituting the plane wave and computing, we obtain:

$$(ik)(ik)\vec{E}_0 e^{i(kx-\omega t)} = \frac{\varepsilon \mu}{c^2} (-i\omega)(-i\omega)\vec{E}_0 e^{i(kx-\omega t)},$$

$$\implies k^2 = \varepsilon \mu \frac{\omega^2}{c^2}, \implies k = \pm n \frac{\omega}{c},$$

where  $n = \sqrt{\varepsilon \mu}$  is the refractive index.

In ordinary dielectrics,  $\varepsilon\mu$  is a positive real number. However, it can also be negative or complex. In those cases, n is complex. Since  $\omega$  is real, the wavenumber is

$$k = \alpha + i\beta$$
,

with  $\alpha, \beta \in \mathbb{R}$ .

Substituting back, we find

$$\vec{E}(x,t) = \vec{E}_0 e^{-\beta x} e^{i(\alpha x - \omega t)},$$

and the intensity is

$$I \propto |\vec{E}|^2 = |\vec{E}_0|^2 e^{-2\beta x}$$
.

Therefore, in media with  $\varepsilon \mu < 0$  or  $\varepsilon \mu \in \mathbb{C}$ , electromagnetic waves cannot propagate: they decay shortly after entering the medium. This is another manifestation of evanescence.<sup>2</sup>

### sez. 2 — Mechanical and Circuit Resonance

Let us frame the following two configurations.

• Consider a body of mass m attached to a spring with elastic constant k and zero rest length, the other end fixed at the origin of a coordinate system. The body is constrained to move along a line, subject to air resistance proportional to its instantaneous velocity, and to an external force  $F_{ext}$ . Newton's second law reads

$$m\frac{\mathrm{d}^2x(t)}{\mathrm{d}t^2} + b\frac{\mathrm{d}x(t)}{\mathrm{d}t} + kx(t) = F_{\mathrm{ext}},$$

where x(t) is the instantaneous position.

• Consider a series circuit with a battery supplying a voltage V, a resistor of resistance R, a capacitor of capacitance C, and an inductor of inductance L. Kirchhoff's law for the circuit gives

$$L\frac{\mathrm{d}^2q(t)}{\mathrm{d}t^2}+R\frac{\mathrm{d}q(t)}{\mathrm{d}t}+\frac{1}{C}q(t)=V,$$

where q(t) is the instantaneous charge on one plate of the capacitor.

 $<sup>^{2}</sup>$ If  $\beta < 0$ , the amplitude instead grows upon entering. This is characteristic of gain (active) media.

From the above, let us observe that the equations governing the two systems are mathematically analogous. This analogy is not accidental: the effective elastic constant of N springs in series/parallel and the effective capacitance of N capacitors in series/parallel are computed in the same way:

$$k_{\text{series}}^{\text{eff}} = \left(\sum_{i=1}^{N} \frac{1}{k_i}\right)^{1}, \qquad k_{\text{parallel}}^{\text{eff}} = \sum_{i=1}^{N} k_i,$$

$$C_{\text{series}}^{\text{eff}} = \left(\sum_{i=1}^{N} \frac{1}{C_i}\right)^{1}, \qquad C_{\text{parallel}}^{\text{eff}} = \sum_{i=1}^{N} C_i.$$

Similarly, mass corresponds to inductance, and mechanical damping corresponds to electrical resistance. Let us therefore study only the mechanical case; the electrical case follows by direct substitution of parameters and variables.

#### 2.1 Damped Harmonic Oscillator

Let us first set  $F_{ext} = 0$ . The governing equation is

$$m\frac{\mathrm{d}^2x}{\mathrm{d}t^2} + b\frac{\mathrm{d}x}{\mathrm{d}t} + kx = 0,$$

with initial conditions  $x(0) = x_0$  and v(0) = 0.

Let us rewrite the equation as

$$\frac{\mathrm{d}^2 x}{\mathrm{d}t^2} + 2\gamma \, \frac{\mathrm{d}x}{\mathrm{d}t} + \omega_0^2 \, x = 0,$$

where  $2\gamma = b/m$  and  $\omega_0^2 = k/m$ . The associated characteristic equation is

$$\lambda^2 + 2\gamma\lambda + \omega_0^2 = 0,$$

with solutions

$$\lambda_{\pm} = -\gamma \pm \sqrt{\gamma^2 - \omega_0^2}.$$

Thus the general solution is

$$x(t) = A e^{-\left(\sqrt{\gamma^2 - \omega_0^2} + \gamma\right)t} + B e^{\left(\sqrt{\gamma^2 - \omega_0^2} - \gamma\right)t},$$

valid for  $\gamma \neq \omega_0$ . Let us distinguish three regimes:

• Case  $\gamma < \omega_0$  (underdamping). Here the exponents are complex, so the solution can be written as

$$\begin{split} x(t) &= A \, e^{-\left(i\sqrt{\omega_0^2 - \gamma^2} + \gamma\right)t} + B \, e^{\left(i\sqrt{\omega_0^2 - \gamma^2} - \gamma\right)t} \\ &= e^{-\gamma t} \left(A \, e^{-i\sqrt{\omega_0^2 - \gamma^2} \, t} + B \, e^{i\sqrt{\omega_0^2 - \gamma^2} \, t}\right) \\ &= C \, e^{-\gamma t} \cos\left(\sqrt{\omega_0^2 - \gamma^2} \, t + \phi\right). \end{split}$$

Imposing the initial conditions yields

$$x(t) = x_0 e^{-\gamma t} \cos\left(\sqrt{\omega_0^2 - \gamma^2} t\right)$$

• Case  $\gamma > \omega_0$  (overdamping). The exponents are real, so the solution is non-oscillatory:

$$x(t) = A e^{-\left(\sqrt{\gamma^2 - \omega_0^2} + \gamma\right)t} + B e^{\left(\sqrt{\gamma^2 - \omega_0^2} - \gamma\right)t}.$$

This brings the mass monotonically to equilibrium at the origin. Imposing the initial conditions gives

 $x(t) = x_0 e^{-\gamma t} \cosh\left(\sqrt{\gamma^2 - \omega_0^2} t\right).$ 

• Case  $\gamma = \omega_0$  (critical damping). The characteristic equation has zero discriminant. Besides the exponential solution  $x_1(t) = C e^{-\gamma t}$ , there is the linearly independent solution

$$x_2(t) = D t e^{-\gamma t}.$$

Hence the general form is

$$x(t) = (C + Dt)e^{-\gamma t}.$$

Using the initial conditions gives

$$x(t) = x_0(1+\gamma t) e^{-\gamma t}.$$

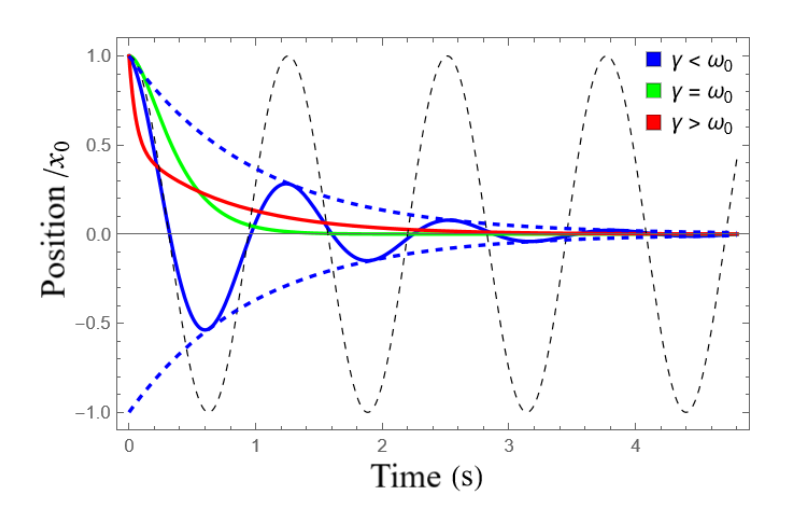


Figure 5: Solutions of the damped oscillator as  $\gamma$  varies. The black dashed curve represents oscillations without damping.

The three regimes are shown in Fig. 5. Let us now ask: why does the  $\gamma = \omega_0$  case produce the fastest decay?

The amplitude decays as:

- $\gamma < \omega_0$ :  $e^{-\gamma t}$ ;
- $\gamma = \omega_0$ :  $e^{-\gamma t}$ ;
- $\gamma > \omega_0$ :  $e^{\left(\sqrt{\gamma^2 \omega_0^2} \gamma\right)t}$ .

Comparing regimes, let us plot the decay exponent versus  $\gamma$ , shown in Fig. 6. From the figure, it is immediate that at  $\gamma = \omega_0$  the exponent is smallest, yielding the fastest decay.

#### 2.2 Damped, Driven Harmonic Oscillator

Let us now introduce a driving force.

<sup>&</sup>lt;sup>3</sup>This is slower because the other exponential decays as  $e^{-(\gamma+\sqrt{\gamma^2-\omega_0^2})t}$ , which dominates at long times.

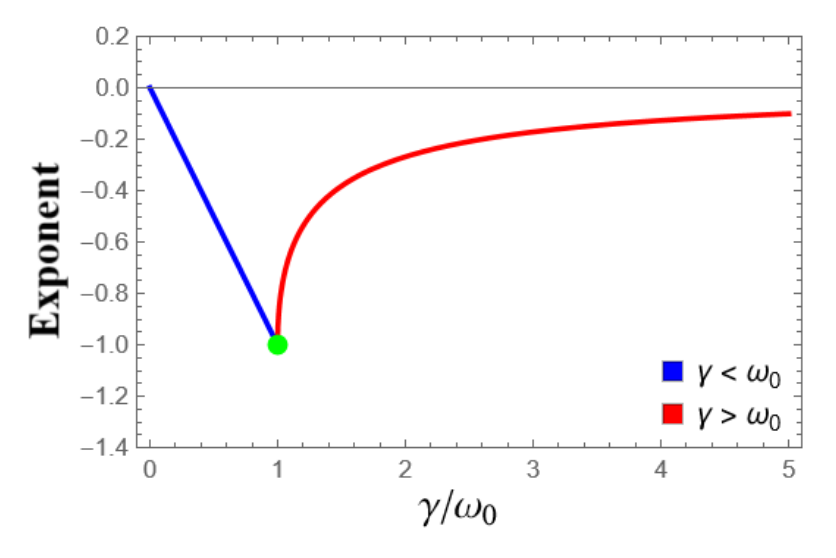


Figure 6: Decay exponent of the amplitude as a function of  $\gamma$ .

Constant force. With  $F_{\text{ext}} = F_0$ , the equation is

$$\frac{\mathrm{d}^2 x}{\mathrm{d}t^2} + 2\gamma \, \frac{\mathrm{d}x}{\mathrm{d}t} + \omega_0^2 \, x = \frac{F_0}{m}.$$

A particular solution is

$$x_p(t) = \frac{F_0}{m\omega_0^2},$$

so the general solution is the homogeneous one shifted by  $x_p$ . One may again split into the three damping regimes and impose initial conditions to fix the constants.

Sinusoidal force. Now consider  $F_{\text{ext}} = F_0 e^{i\omega t}$ . The equation is

$$\frac{\mathrm{d}^2 x}{\mathrm{d}t^2} + 2\gamma \frac{\mathrm{d}x}{\mathrm{d}t} + \omega_0^2 x = \frac{F_0}{m} e^{i\omega t}.$$

Let us try the ansatz  $x(t) = Ae^{i\omega t}$ . Substituting, we find

$$\left(-\omega^2+2i\gamma\omega+\omega_0^2\right)\mathcal{A}e^{i\omega t}=\frac{F_0}{m}e^{i\omega t}.$$

Thus,

$$\mathcal{A}(\omega) = \frac{F_0/m}{\omega_0^2 - \omega^2 + 2i\gamma\omega}.$$
 (2.1)

Writing  $\mathcal{A} = \rho e^{i\theta}$  in polar form, we obtain

$$\rho = \frac{F_0/m}{\sqrt{(\omega_0^2 - \omega^2)^2 + 4\gamma^2 \omega^2}}, \qquad \tan\theta = -\frac{2\gamma\omega}{\omega_0^2 - \omega^2}.$$

Thus the steady-state solution is

$$x_p(t) = \frac{F_0/m}{\sqrt{(\omega_0^2 - \omega^2)^2 + 4\gamma^2 \omega^2}} \cos \left[\omega t - \arctan\left(\frac{2\gamma\omega}{\omega_0^2 - \omega^2}\right)\right].$$

The full solution is the sum of the homogeneous transient and this periodic response. Since the homogeneous part decays with time, the long-time behavior is purely periodic. Examples are shown in Fig. 7.

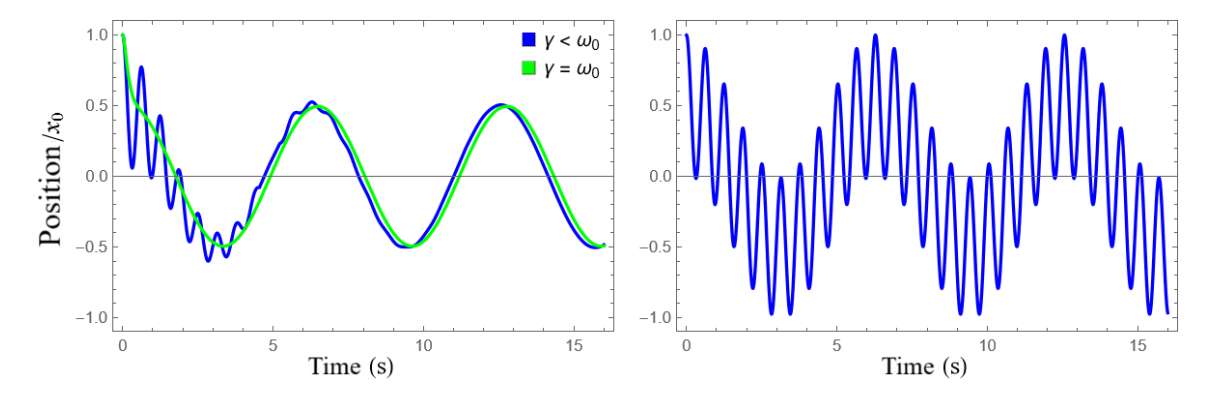


Figure 7: Damped, driven harmonic oscillator. Left:  $\gamma < \omega_0$  and  $\gamma = \omega_0$ . The case  $\gamma > \omega_0$  is omitted, as it is qualitatively identical to  $\gamma = \omega_0$ . Right: undamped case.

**Resonance.** Let us now examine the amplitude as a function of  $\omega$  and  $\gamma$ . From the expression above, the amplitude peaks near  $\omega_0$ , producing the phenomenon of *resonance*, widespread in mechanical, acoustic, electronic,<sup>4</sup> and electromagnetic systems.<sup>5</sup>

When the driving frequency is close to the natural frequency, the force is in phase with the displacement, so the amplitude grows. In the ideal undamped case, the amplitude diverges.

The maximum can be found by minimizing the denominator:

$$\frac{\mathrm{d}}{\mathrm{d}\omega} \left[ (\omega_0^2 - \omega^2)^2 + 4\gamma^2 \omega^2 \right] = 0 \quad \Longrightarrow \quad \omega^* = 0, \sqrt{\omega_0^2 - 2\gamma^2}.$$

Thus, if  $\gamma < \omega_0/\sqrt{2}$  the maximum occurs at  $\omega = \sqrt{\omega_0^2 - 2\gamma^2}$ , otherwise at  $\omega = 0$ . The peak amplitude is

$$\mathcal{A}_{\text{max}} = \frac{F_0}{m\omega_0^2}, \quad \frac{F_0/m}{2\gamma\sqrt{\omega_0^2 - \gamma^2}},$$

which diverges as  $\gamma \to 0$ .

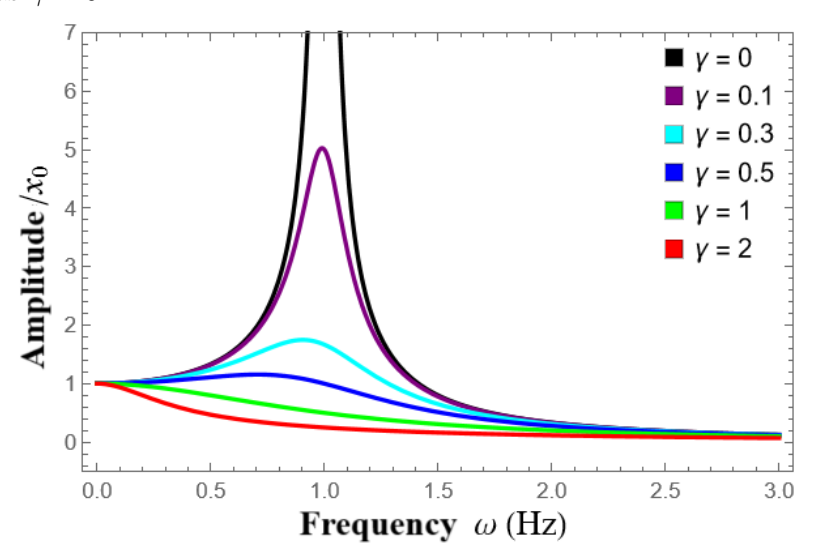


Figure 8: Oscillation amplitude as a function of  $\omega$ , for different damping values  $\gamma$ , with  $\omega_0=1\,\mathrm{Hz}$  and  $F_0/m=1\,\mathrm{m/s^2}$ .

<sup>&</sup>lt;sup>4</sup>Radios exploit resonance: tuning the capacitance of the internal circuit adjusts its resonance frequency to match that of the incoming electromagnetic wave from a radio station, thereby maximizing response.

<sup>&</sup>lt;sup>5</sup>The *Lorentz oscillator* model of charges in a dielectric under an oscillating electric field has exactly this form, with the dielectric function  $\varepsilon(\omega)$  exhibiting a resonance.

## sez. 3 — Snell's Law in Every Flavor

Snell's law for light rays relates incidence and refraction angles at the interface between two media with refractive indices:

$$n_1 \sin \theta_i = n_2 \sin \theta_r$$
.

If  $n_1 > n_2$ , depending on the incidence angle, total internal reflection can occur. Since the refraction angle is

$$\theta_r = \arcsin\left(\frac{n_1}{n_2}\sin\theta_i\right),$$

this relation implies that  $\theta_r$  can equal  $\pi/2$  even if  $\theta_i < \pi/2$ , because the index ratio is greater than one. Therefore, if the incidence angle exceeds

$$\theta_{\text{max}} = \arcsin \frac{n_2}{n_1},$$

the ray is not transmitted into the second medium.

If the refractive index varies along x, the quantity

$$n(x)\sin\theta(x)$$

is constant along the ray path. This is called the *Snell invariant*. If n(x) is a decreasing function, the ray may undergo total internal reflection. If n(x) is an increasing function, rays tend to become parallel to the x-axis.

As for spherically symmetric media, the Snell invariant takes a slightly different form.

Theorem (Snell Invariant in Spherically Symmetric Media). The Snell invariant for spherically symmetric media is

$$n(r) r \sin \theta(r)$$
,

where r is the radial coordinate and  $\theta$  the angle between the ray direction and the radial direction.

*Proof.* Let us split space into infinitely many concentric spherical shells of infinitesimal thickness, within each of which n(r) may be considered constant. By Snell's law across two consecutive shells,

$$n_1 \sin \theta_1 = n_2 \sin \theta_2$$
.

By the exterior angle theorem,

$$\theta_2 = \theta_2' + \delta\theta$$
.

Therefore,

$$\sin \theta_2 = \sin \theta_2' \cos \delta \theta + \cos \theta_2' \sin \delta \theta \approx \sin \theta_2' + \cos \theta_2' \delta \theta.$$

Substituting into Snell's law and passing to the infinitesimal limit,

$$n_1 \sin \theta_1 = n_2 \sin \theta_2' + n_2 \cos \theta_2' d\theta.$$

From this, we obtain

$$d(n\sin\theta) = -n\cos\theta d\theta = -\frac{n}{r}\frac{dr}{dl}rd\theta = -n\frac{dr}{r}\sin\theta.$$

Hence,

$$r d(n\sin\theta) + n\sin\theta dr = 0,$$

$$d(n(r)r\sin\theta)=0.$$

Thus  $n(r) r \sin \theta$  is uniform along the ray trajectory.

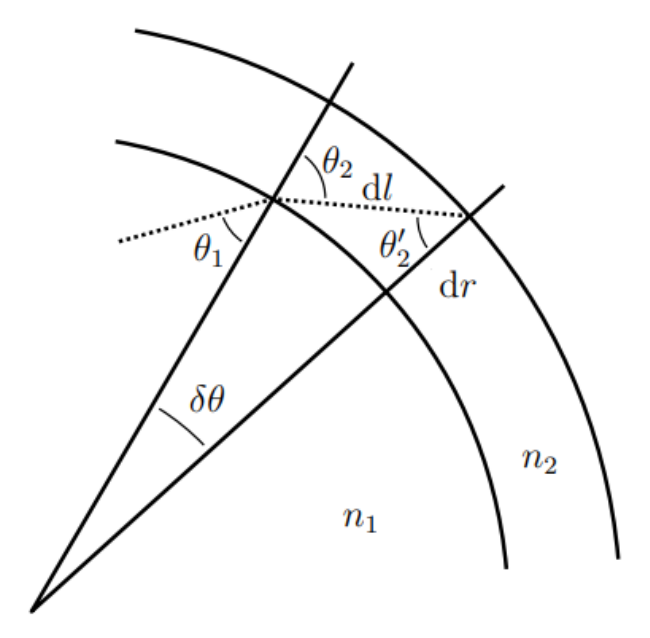


Figure 9: Ray trajectory between two spherical shells in a medium with a spherically symmetric refractive index.

An analogous version of Snell's law holds for mechanical waves, such as sound in air or seismic waves in the ground. For waves propagating between two media,

$$\frac{\sin \theta_i}{v_1} = \frac{\sin \theta_r}{v_2},$$

where  $v_1$  and  $v_2$  are the respective wave speeds (e.g. the speed of sound). In this case, the Snell invariant in an inhomogeneous medium is

$$\frac{\sin\theta(x)}{v(x)}.$$

Sound waves produced at Earth's surface travel through the atmosphere in all directions. Let us note that upward-going waves bend because the speed of sound decreases with altitude, depending on temperature and air density. Thus sound waves also refract and can undergo total internal reflection.

Example 3.1 (Apparent Position of Stars, from SNS admission exam (2014)). The atmosphere's refractive index increases continuously from its highest layer, where n = 1, to the surface, where n = 1,0003. Express the relation between angles  $\theta_{true}$  and  $\theta_{apparent}$ , where  $\theta_{true}$  defines the true direction of light from a star, while  $\theta_{apparent}$  defines the direction as perceived by an observer on the surface. Ignore Earth's curvature.

Let us divide the atmosphere into infinitely many layers of infinitesimal thickness, as sketched in Fig. 10. Within each layer the refractive index is homogeneous, so the ray segment is straight.

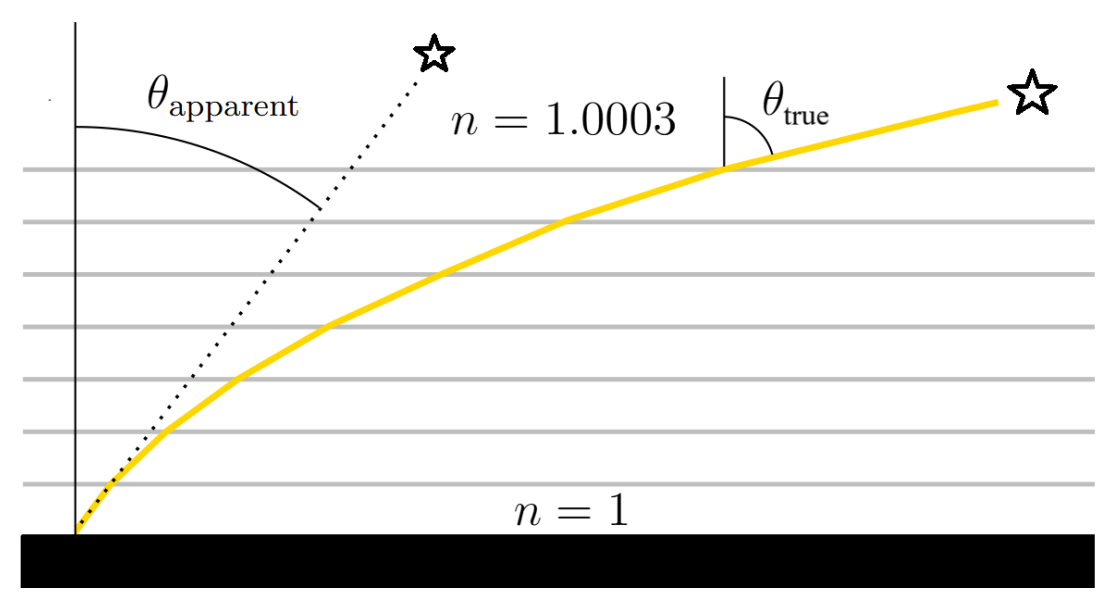


Figure 10: Deviation of a light ray through the atmosphere, modeled as infinitely many layers.

Then Snell's law applies across each interface:

$$\begin{split} n_0 \sin \theta_0 &= n_1 \sin \theta_1, \\ n_1 \sin \theta_1 &= n_2 \sin \theta_2, \\ n_2 \sin \theta_2 &= n_3 \sin \theta_3, \\ &\vdots \\ n_{k-1} \sin \theta_{k-1} &= n_k \sin \theta_k, \\ n_k \sin \theta_k &= n_{\text{vacuum}} \sin \theta_{\text{vacuum}}. \end{split}$$

This chain relation implies

$$n_0 \sin \theta_0 = n_{\text{vacuum}} \sin \theta_{\text{vacuum}}$$
.

At the surface  $n_0=1{,}0003$ , while in vacuum  $n_{\rm vacuum}=1$ . Identifying  $\theta_0=\theta_{\rm apparent}$  and  $\theta_{\rm vacuum}=\theta_{\rm true}$ , we find

$$1,0003 \cdot \sin \theta_{\text{apparent}} = \sin \theta_{\text{true}},$$

$$\implies \quad \theta_{\rm apparent} = \arcsin\left(\frac{\sin\theta_{\rm true}}{1.0003}\right) < \theta_{\rm true}.$$

Thus observers perceive stars slightly higher in the sky than their true positions. For the same reason, one can see stars that have not yet actually risen.

#### 3.1 Derivation of Snell's Law

Let us now derive Snell's law from Fermat's principle.

For isotropic media, the travel time of a path element ds is

$$dt = \frac{ds}{v(\mathbf{r})} = n(\mathbf{r}) \frac{ds}{c},$$

with  $n(\mathbf{r}) \geq 0$  for all  $\mathbf{r}$ . Hence the travel time is

$$T = \int_{S_A}^{S_B} n(\mathbf{r}) \, \frac{\mathrm{d}s}{c}.$$

Generally, physical systems minimize some quantity. Here, light follows the path that minimizes the travel time between two points. Therefore, let us minimize

$$F \equiv n(\mathbf{r}) \, \mathrm{d}s$$

where ds depends on the chosen coordinates.

Let us use Cartesian coordinates and suppose  $n(\mathbf{r}) = n(z)$ . Restricting to the xz-plane, the infinitesimal length element is

$$ds = \sqrt{(dx)^2 + (dz)^2} = \sqrt{1 + z'^2} dx.$$

Thus the function to minimize is

$$F = n(z)\sqrt{1 + z'^2}.$$

According to the Euler–Lagrange equations, when F does not explicitly depend on x, the quantity

 $F - z' \frac{\partial F}{\partial z'}$ 

remains constant. In this case,

Constant = 
$$n(z)\sqrt{1+z'^2} - \frac{n(z)z'^2}{\sqrt{1+z'^2}} = \frac{n(z)}{\sqrt{1+z'^2}}$$
. (3.1)

Since

$$\sin\theta = \frac{1}{\sqrt{1 + \tan^2\theta}},$$

we recover the Snell invariant.

Equation (3.1) thus gives ray trajectories in the medium:

$$\frac{\mathrm{d}z}{\mathrm{d}x} = \sqrt{\frac{n^2(z)}{k^2} - 1}.$$

The constant k is fixed by the initial conditions, such as the ray's orientation at a given point. Conversely, if we prescribe a trajectory z(x), we may use this equation to deduce the refractive index n(z) that produces it.

Phenomena such as mirages follow directly: in deserts, the refractive index varies rapidly with altitude due to temperature gradients, bending rays so that objects appear displaced and distorted.

**Example 3.2** (Trajectories in a Special Case). In the desert, the refractive index depends on height as  $n(z) = n_0 \sqrt{1 + z/h}$ . Find z(x) for a ray leaving from A = (0, h) and reaching an observer at B = (h, h).

In this case, one possible trajectory is the straight-line segment joining A and B,<sup>6</sup> which indeed satisfies Eq. (3.1).

The nontrivial solution follows from

$$\frac{\mathrm{d}z}{\mathrm{d}x} = \sqrt{\alpha \left(1 + \frac{z}{h}\right) - 1},$$

where  $\alpha \equiv n_0^2/k^2$ . Separating variables and integrating,

$$\frac{2h}{\alpha}\sqrt{\alpha - 1 + \alpha \frac{z}{h}} = x + \beta,\tag{3.2}$$

<sup>&</sup>lt;sup>6</sup>One must explicitly note this possibility, since trajectories with constant dependent variable are subtle. The same occurs in the spherically symmetric case, where circles at constant r can cause confusion.

with  $\beta$  an integration constant.

Thus the general trajectory is

$$z(x) = \frac{\alpha}{4h} (x+\beta)^2 + \frac{h}{\alpha} (1-\alpha).$$

Imposing that both A and B lie on the trajectory, we obtain

$$\alpha = 8\left(2 \pm \sqrt{\frac{15}{4}}\right), \qquad \beta = -\frac{h}{2}.$$

The (+) solution is unphysical, since the corresponding parabola dips to z < 0 within the interval [0, h].

#### 3.2 Inferior and Superior Mirages

Sometimes mirages cause the apparent position of objects to lie below the true one (inferior mirages), and other times above (superior mirages). Let us analyze this feature, tied to the concavity of trajectories.

Differentiating both sides of Eq. (3.1) with respect to x, we obtain:

$$0 = \frac{\mathrm{d}n(z)}{\mathrm{d}z} \frac{z'}{\sqrt{1+z'^2}} - \frac{n(z)z'z''}{(\sqrt{1+z'^2})^3}$$
$$= z' \left(\sqrt{1+z'^2}\right)^{-3} \left[n'(z)\left(1+z'^2\right) - n(z)z''\right].$$

Thus, apart from the trivial case of rays parallel to x, we obtain  $n'(z)(1+z'^2) = n(z)z''$ , showing that n'(z) and z'' share the same sign.

Therefore:

- Inferior mirages:  $z'' > 0 \Longrightarrow n'(z) > 0$ . This occurs when air temperature decreases with altitude, as in desert mirages;
- Superior mirages:  $z'' < 0 \Longrightarrow n'(z) < 0$ . This occurs when air temperature increases with altitude, as in the Fata Morgana observed at sea.

Fig. 11 illustrates both cases.

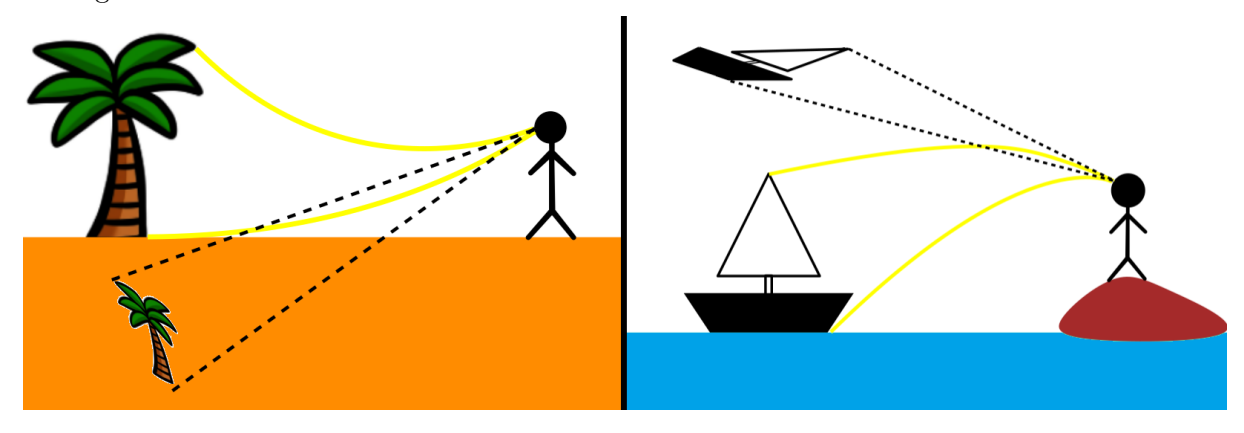


Figure 11: Inferior mirage in the desert (left) and superior mirage at sea (right). Dashed lines indicate ray tangents at the observer's eye. Images appear distorted because of ray curvature.

## 

The orbits of point masses subject to radial forces can be determined by solving Binet's equation:

$$\frac{\mathrm{d}^2}{\mathrm{d}\theta^2} \left( \frac{1}{r(\theta)} \right) + \frac{1}{r(\theta)} = -\frac{m \, r^2(\theta)}{L^2} \, F(r, \theta), \tag{4.1}$$

where m is the orbiting mass, L the angular momentum about the force center,  $r(\theta)$  the polar equation of the orbit, and  $F(r,\theta)$  the magnitude of the radial force.<sup>7</sup> The resulting orbit is a plane curve, which need not be closed (e.g., spirals) and need not be bounded (spirals, parabolas, hyperbolas).

Example 4.1 (Null Force). Here Binet's equation reduces to

$$\frac{\mathrm{d}^2}{\mathrm{d}\theta^2} \left( \frac{1}{r(\theta)} \right) + \frac{1}{r(\theta)} = 0,$$

whose solution is

$$\frac{1}{r(\theta)} = A\cos\theta + B\sin\theta,$$

with constants A, B fixed by the requirement that the curve pass through a given point with a specified direction. In any case, this describes a straight line in polar coordinates, consistent with the fact that a body subject to no force moves along a straight trajectory.

Example 4.2 (Gravitational Orbits). For gravity, Eq. (4.1) becomes

$$\frac{\mathrm{d}^2}{\mathrm{d}\theta^2} \left( \frac{1}{r(\theta)} \right) + \frac{1}{r(\theta)} = \frac{GMm^2}{L^2},$$

where M is the mass of the attractor, fixed at the origin.

Let us first solve the homogeneous equation

$$\frac{\mathrm{d}^2}{\mathrm{d}\theta^2} \left( \frac{1}{r(\theta)} \right) + \frac{1}{r(\theta)} = 0,$$

whose solution is

$$\frac{1}{r(\theta)} = A\cos\theta + B\sin\theta.$$

A particular solution is

$$\frac{1}{r(\theta)} = \frac{GMm^2}{L^2}.$$

Thus the general solution is

$$\frac{1}{r(\theta)} = A\cos\theta + B\sin\theta + \frac{GMm^2}{L^2}.$$

$$\frac{\mathrm{d}^2 u(\theta)}{\mathrm{d}\theta^2} + u(\theta) = -\frac{m}{L^2} \frac{\mathrm{d}}{\mathrm{d}u} \left[ V\left(\frac{1}{u}\right) \right],\tag{4.2}$$

with  $u(\theta) \equiv r^{-1}(\theta)$  and V the potential energy associated with  $\vec{F} = -\nabla V$ . This alternative form requires the additional assumption of a potential depending only on r, i.e., that the force is central. Under these conditions one can also prove that allowable orbits are symmetric about an axis through the force center.

<sup>&</sup>lt;sup>7</sup>Textbooks and online sources usually state that Binet's equation holds for central forces. In fact it applies to radial forces, which include central ones. This is because Eq. (4.1) is derived using angular momentum conservation, valid for any radial field. There is no assumption that the force must be conservative. Other versions exist, such as

This implies

$$r(\theta) = \frac{L^2/GMm^2}{A\cos\theta + B\sin\theta + 1},$$

with A, B redefined.

By choosing the orbit's orientation, we can reduce to

$$r(\theta) = \frac{L^2/GMm^2}{1 + \varepsilon \cos \theta},\tag{4.3}$$

where  $\varepsilon$  is the eccentricity. As  $\varepsilon$  varies over  $[0, \infty)$ , Eq. (4.3) generates the four conic sections: circle, ellipse, parabola, and hyperbola.

**Example 4.3** (Cardioid). Which force produces a cardioidal orbit? The polar equation in Fig. 12 is

$$r(\theta) = R(1 + \cos \theta),$$

with R a characteristic length.

Substituting into Eq. (4.1), we obtain

$$F(r) = -\frac{3RL^2}{m r^4} \propto -r^{-4},$$

an attractive central force.

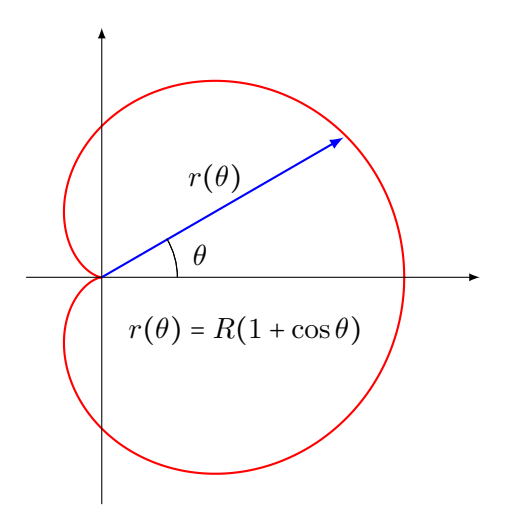


Figure 12: Cardioid orbit.

What about optics? Light rays can also trace orbits—sometimes even closed ones—if the refractive index n of the medium varies with position  $\vec{r}$ . Let us restrict to spherically symmetric indices,  $n(\vec{r}) = n(r)$ . In this case, the trajectory lies in a plane, just as in radial force fields, and can be described in polar coordinates.

The relation between trajectory  $r(\theta)$  and n(r) admits several equivalent forms. Two useful ones are:

$$\frac{\mathrm{d}^2}{\mathrm{d}\theta^2} \left( \frac{1}{r(\theta)} \right) + \frac{1}{r(\theta)} = -\frac{r^2(\theta)}{2k^2} \frac{\mathrm{d}}{\mathrm{d}r} \left[ n^2(r) \right], \tag{4.4}$$

$$\frac{\mathrm{d}^2 u(\theta)}{\mathrm{d}\theta^2} + u(\theta) = \frac{1}{2k^2} \frac{\mathrm{d}}{\mathrm{d}u} \left[ n^2 \left( \frac{1}{u} \right) \right],\tag{4.5}$$

with  $u(\theta) \equiv r^{-1}(\theta)$  and  $k^2$  a positive integration constant.

Let us notice how Eq. (4.5) resembles Eq. (4.2), which is valid only for central forces. Moreover, if the refractive index is homogeneous, the analogy with a free body is exact: a ray in a homogeneous medium is a straight line. But straight lines are not the only trajectories in common. In fact, there are infinitely many.

Let us compare Eq. (4.1) and Eq. (4.4). Their left-hand sides are identical. Consider a central force

$$\vec{F}(r) = \alpha r^{\beta} \hat{r},$$

and a spherically symmetric index

$$n(r) = \gamma r^{\delta},$$

with  $\gamma > 0$ .

The corresponding right-hand sides become

$$-\frac{m\alpha}{L^2}r^{\beta+2}$$
 and  $-\frac{\delta\gamma^2}{k^2}r^{2\delta+1}$ .

Hence the optical trajectories match the mechanical orbits if

$$\delta \to \frac{\beta+1}{2}, \qquad \gamma \to \frac{k}{L} \sqrt{\frac{2m\alpha}{\beta+1}}.$$

Recall that this requires  $\alpha/(\beta+1)>0$ .

For instance, optical trajectories are conics for  $\delta = -1/2$ , corresponding to gravity with  $\beta = -2$ . Straight lines are recovered with  $\alpha = \gamma = 0$ , or with  $\delta = 0$ .

Equations (4.4) and (4.5) are not always convenient. An alternative is

$$n^{2}(r) = \frac{k^{2}}{r^{4}} \left[ r^{2} + \left(\frac{\mathrm{d}r}{\mathrm{d}\theta}\right)^{2} \right],\tag{4.6}$$

from which we may infer properties of  $k^2$ . Rewriting,

$$k^{2} = n^{2}(r) r^{2} \frac{r^{2} (d\theta)^{2}}{r^{2} (d\theta)^{2} + (dr)^{2}}.$$

The fraction is exactly the sine squared of the angle  $\phi$  between the ray direction and the radial direction. Therefore,

$$k = n(r) r \sin \phi. \tag{4.7}$$

This is precisely the Snell invariant for a spherically symmetric refractive index. Its structure mirrors the magnitude of a particle's angular momentum about the center of a radial force field:

$$L = m v(r) r \sin \phi$$

where  $\phi$  is the angle between the velocity and the radial direction.

We deduce that Eq. (4.7) expresses conservation of the light ray's angular momentum.<sup>8</sup>

Finally, comparing Eq. (4.2) and Eq. (4.5), we see that the transformations  $k^2 \leftrightarrow L^2/2m$  and  $n^2 \leftrightarrow E - V$  identify the two forms, where E is a constant since derivatives of  $n^2$  and -V must match. Applying these substitutions to Eq. (4.6), we obtain

$$E - V(r) = \frac{L^2}{2m r^4} \left[ r^2 + \left(\frac{\mathrm{d}r}{\mathrm{d}\theta}\right)^2 \right] = \frac{L^2}{2m r^2} + \frac{1}{2} m \left(\frac{\mathrm{d}r}{\mathrm{d}t}\right)^2,$$

where angular momentum conservation has been used.

Thus, we have recovered the conservation of energy in a central force field.

<sup>&</sup>lt;sup>8</sup>The photon momentum is  $p = h/\lambda = hf/v = hfn/c$ , where v = c/n is the speed of light in the medium. The photon's angular momentum about the symmetry center is  $L = |\vec{r} \times \vec{p}| = hfn(r)r\sin\phi/c$ . Since the frequency does not change across media, conservation of the quantity in Eq. (4.7) is directly analogous to angular momentum conservation.

### sez. 5 — Orbit Decay

Every physical system exhibits dissipation—the conversion of mechanical or electrical energy into heat. Common causes include friction, inelastic collisions, and electrical resistance. Let us now present two noteworthy examples, one at planetary scale and the other at atomic scale, in which the systems evolve in a strikingly similar way due to energy loss, though the underlying mechanisms differ radically.

**Example 5.1** (The Satellite Paradox). A satellite of mass m initially moves on a circular orbit of radius  $R_0$  around a point-like body of mass  $M \gg m$ . The satellite is subject to a drag force  $\vec{F}_a = -A|\vec{v}|\vec{v}$ . Assuming the drag is small enough to approximate the orbit as instantaneously circular, find r(t), i.e., the satellite's distance from the planet as a function of time. How long does it take for the satellite to hit the surface?  $\uparrow$ 

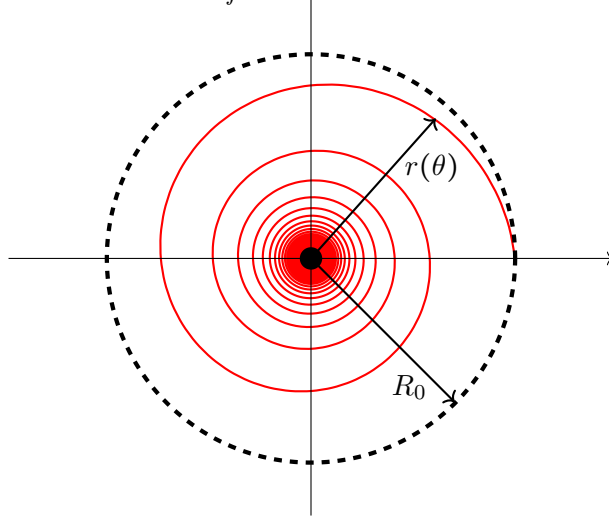


Figure 13: Satellite trajectory. The spiral is exaggerated for clarity and does not strictly satisfy the instantaneously circular approximation.

Let us write the energy balance:

$$\frac{\mathrm{d}E}{\mathrm{d}t} = \vec{v} \cdot \vec{F}_a = -Av^3.$$

The system's mechanical energy is

$$E = -\frac{GMm}{2r(t)},$$

so that

$$\frac{GMm}{2r^2(t)}\frac{\mathrm{d}r}{\mathrm{d}t} = -Av^3.$$

Let us now use the suggested approximation: if the orbit is instantaneously circular, the radial velocity is approximately zero, while the orbital speed is  $v = \sqrt{GM/r}$ . Substituting, we obtain a separable first-order ODE:

$$r^{-\frac{1}{2}}\frac{\mathrm{d}r}{\mathrm{d}t} = -\frac{2A}{m}(GM)^{\frac{1}{2}}.$$

Integrating, we find

$$r(t) = R_0 \left[ 1 - \frac{A}{m} \left( \frac{GM}{R_0} \right)^{\frac{1}{2}} t \right]^2.$$

Let us note that r(t) decreases monotonically—drag shrinks the orbit. Smaller orbits correspond to more tightly bound systems, i.e., lower (more negative) total energy. And what does the drag do? It reduces the system's energy. Everything is consistent.

The time to reach r = 0 is

$$t_{\text{fall}} = \frac{m}{A} \left( \frac{R_0}{GM} \right)^{\frac{1}{2}} = \frac{m}{Av_0},$$

where  $v_0$  is the initial orbital speed.

So, where lies the paradox? We said r(t) decreases, so

$$v(t) = \sqrt{GM/r(t)}$$

increases! How can speed increase in the presence of drag? It can, because drag is not the only force—gravity also acts. Dissipative forces certainly decrease the system's mechanical energy (as here), but they do not necessarily decrease the kinetic energy. They decrease it only if they are the sole forces doing work.<sup>9</sup> Thus there is no paradox.

For practice, let us also compute how many revolutions the satellite makes and how far it travels before crashing. If divergences occur at r = 0, give the planet a finite radius  $0 < R_p < R_0$ . For the path length, recall the formula for the length of a polar curve. Finally, try to derive the explicit trajectory  $r(\theta)$ .

**Example 5.2** (Breakdown of the Rutherford Atom). Classical electromagnetism cannot explain the phenomena that occur when electric charges are bound in atoms. In particular, the theory predicts that an accelerating charged particle radiates energy as electromagnetic waves. The radiated power of a charge q with acceleration a in vacuum, in the non-relativistic regime, is

$$P = \frac{q^2 a^2}{6\pi\varepsilon_0 c^3},$$

where c is the speed of light. Model the hydrogen atom as a proton fixed in space with an electron orbiting around it. Because of energy loss, the electron spirals inward and eventually hits the proton. If the initial orbital radius is  $R_0$ , find the time after which the electron collides with the proton, assuming the orbit remains approximately circular at all times.

Let us again assume that the orbital radius changes little per revolution, so that the orbit can be considered instantaneously circular. Then

$$F_{\rm el} = m_e \frac{v^2}{r} \quad \Longrightarrow \quad \frac{1}{4\pi\varepsilon_0} \frac{e^2}{r^2} = m_e \frac{v^2}{r},$$

which allows us to express  $v^2$  as a function of r. From this we can compute the kinetic energy. The potential energy is

$$U = -\frac{1}{4\pi\varepsilon_0} \frac{e^2}{r}.$$

Adding both contributions yields

$$E(r) = -\frac{1}{8\pi\varepsilon_0} \frac{e^2}{r}, \qquad \frac{\mathrm{d}E}{\mathrm{d}r} = \frac{1}{8\pi\varepsilon_0} \frac{e^2}{r^2}.$$

<sup>&</sup>lt;sup>9</sup>One might be tempted to think gravity does no work here, since in circular orbits displacement is always tangential and never radial. In reality, despite the instantaneously circular approximation, we are still assuming gravity does work: we take  $v(t) = \sqrt{GM/r(t)}$  at each instant. However slowly, the satellite drifts inward, so gravity performs positive work.

According to Larmor's formula, the radiated power is

$$P = \frac{\mathrm{d}E}{\mathrm{d}t} = -\frac{e^2 a^2}{6\pi\varepsilon_0 c^3},$$

with the minus sign reminding us that energy is lost. The acceleration, centripetal under our assumptions, is

$$a = \frac{1}{4\pi\varepsilon_0} \frac{e^2}{m_e r^2}.$$

Let us write the energy-balance equation:

$$-\frac{e^2}{6\pi\varepsilon_0 c^3} \left( \frac{1}{4\pi\varepsilon_0} \frac{e^2}{m_e r^2} \right)^2 = \frac{1}{8\pi\varepsilon_0} \frac{e^2}{r^2} \frac{\mathrm{d}r}{\mathrm{d}t}.$$

After simplification, this gives a first-order separable ODE:

$$\frac{\mathrm{d}r}{\mathrm{d}t} = -\frac{e^4}{12\pi^2 m_e^2 \varepsilon_0^2 c^3} \frac{1}{r^2}.$$

Integrating,

$$\int_{R_0}^{0} r^2 dr = \int_{0}^{\tau} -\frac{e^4}{12\pi^2 m_e^2 \varepsilon_0^2 c^3} dt,$$

$$\implies \tau = \frac{4\pi^2 m_e^2 \varepsilon_0^2 c^3 R_0^3}{e^4}.$$

Substituting numerical constants gives a collapse timescale of order  $10^{-11}$  s—clearly unrealistic. According to classical physics, atoms should not exist. After Rutherford, Bohr "patched" the theory by postulating stationary orbits. The true resolution came later with the quantum theory of de Broglie, Schrödinger, & company.

## 

#### 6.1 Electric Field and Velocity Field

Consider a point charge q in vacuum, placed at the origin. The electric field and potential it generates are

$$\vec{E}(\vec{r}) = \frac{q}{4\pi\varepsilon_0 r^2} \hat{r} \qquad \varphi_E(\vec{r}) = \frac{q}{4\pi\varepsilon_0 r} \quad \text{in 3D},$$

$$\vec{E}(\vec{r}) = \frac{q}{2\pi\varepsilon_0 r} \hat{r} \qquad \varphi_E(\vec{r}) = -\frac{q}{2\pi\varepsilon_0} \ln\left(\frac{r}{r_0}\right) = -\frac{q}{2\pi\varepsilon_0} \ln r + C \quad \text{in 2D}$$

where  $r_0$  is a given distance from the origin and C is a constant.<sup>10</sup> The dimensional dependence follows from Gauss's theorem: since the flux through any closed surface enclosing the charge is  $q/\varepsilon_0$ , we have

$$\vec{E}(\vec{r}\,) = \frac{q}{\varepsilon_0 S(r)}\,\hat{r},$$

where S is the surface area of the sphere centered on the charge. In 2D the "sphere" reduces to a circle, so the field must differ from the 3D case.

 $<sup>^{10}</sup>$ Yes, strictly speaking it is not correct to drop  $r_0$  in the denominator because the logarithm's argument would carry dimensions. However, doing so helps to simplify the notation in exercises.

An analogous story holds in fluid dynamics for irrotational flows of incompressible inviscid fluids. There, one deals with sources/sinks rather than positive/negative charges. In this case, the "strength" of the source/sink is the flow rate F entering/leaving it, i.e., the volume injected into or removed from the system per unit time. By analogy with the electrostatic case, the velocity field and potential of a source at the origin are

$$\vec{v}(\vec{r}) = \frac{F}{4\pi r^2} \hat{r} \qquad \varphi_V(\vec{r}) = \frac{F}{4\pi r} \quad \text{in 3D},$$

$$\vec{v}(\vec{r}) = \frac{F}{2\pi r} \hat{r} \qquad \varphi_V(\vec{r}) = -\frac{F}{2\pi} \ln\left(\frac{r}{r_0}\right) = -\frac{F}{2\pi \varepsilon_0} \ln r + C \quad \text{in 2D}.$$

Thus a potential can be associated with the velocity as well. This is because in the present setting both the electrostatic field and the velocity field are irrotational. One must also specify that this holds only for incompressible fluids; this hypothesis is needed to apply flow-rate conservation on the Gaussian surface.

We can now infer what happens if a source and a sink are present in space: such a configuration is a dipole! The velocity distribution in space is shown in Fig. 14 and is identical to that of an electric dipole.

If we have N sources and sinks in unbounded space, in the absence of other objects and forces, we can find the velocity at any point by simple superposition. But what if the available space is limited or obstacles are present? A simple vector sum no longer suffices. Again, the analogy with electrostatics comes to the rescue.

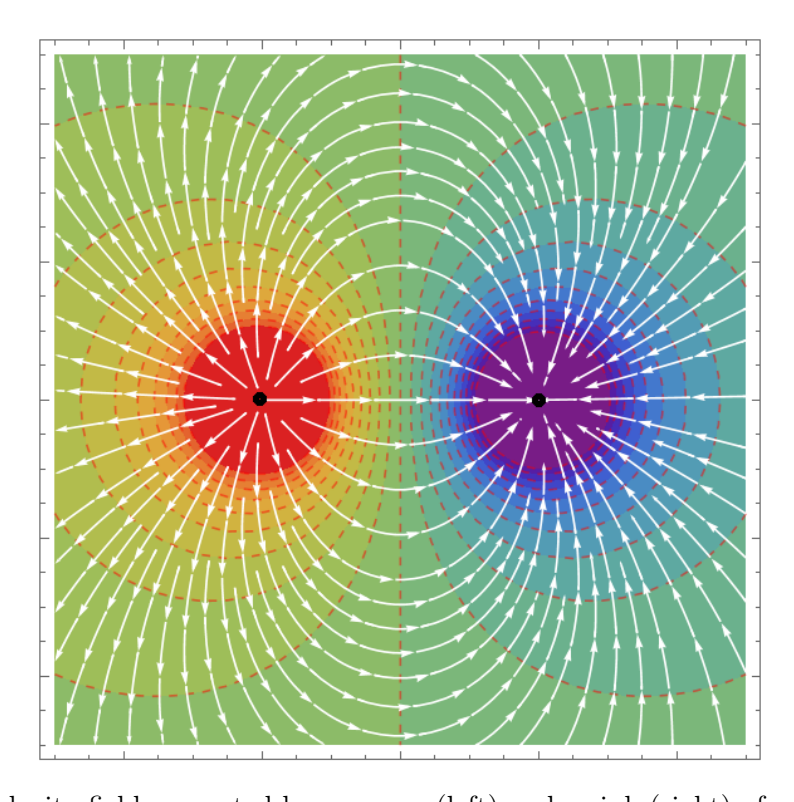


Figure 14: Velocity field generated by a source (left) and a sink (right) of equal strength.

#### 6.2 Method of Images

In electrostatics, when dealing with charge distributions near conductors, we use the well-known method of images. For example, the field of a point charge q placed at distance d from the

<sup>&</sup>lt;sup>11</sup>Velocity fields can of course be rotational—think of whirlwinds! However, if we restrict attention to point sources, vortices do not form spontaneously.

center of a grounded conducting sphere of radius R < d is identical to the field of the configuration consisting of the same charge and an image charge -qR/d placed at a distance  $R^2/d$  from the center of the sphere, as illustrated in Fig. 15. Why is this true? Answering that is tantamount to explaining how and why the method of images works.

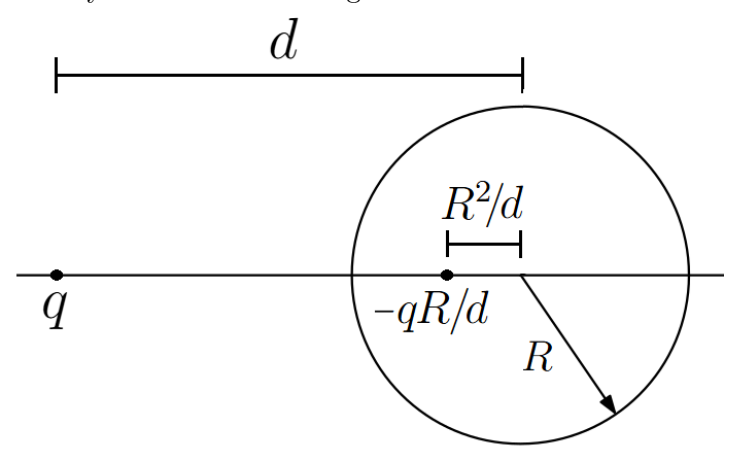


Figure 15: Placement of the image charge for the grounded conducting sphere problem.

The Electrostatics Problem. Consider fixed external charges in a system containing dielectric or conducting objects, which may be both charged or uncharged. At any point in space, the electric field is the vector sum of the field due to the external charges and the field due to charges induced in the objects by the former. For instance, bringing a point charge close to a neutral dielectric sphere produces polarization charges on the sphere, whose field superposes with that of the original charge. In general, such problems are analytically difficult to deal with. Closed-form solutions exist only for highly symmetric bodies—spheres, infinitely long cylinders, infinite planes—where the method of images is particularly useful.

Method of Images. The configuration just described is governed by a Poisson equation for the electric potential  $\varphi_E$  together with boundary conditions. For conductors, the electric field immediately outside must be perpendicular to the surface, which is equivalent to the statement that the potential is constant everywhere inside and on the surface of a conductor. Once the boundary conditions are determined, the uniqueness theorem for Poisson's equation comes into play.

Theorem (Uniqueness). In a connected region of space, the electric field generated by given charges and fixed media is uniquely determined by the geometry of the system and the boundary conditions.

Therefore, once a potential  $\varphi_E$  is found that solves Poisson's equation and satisfies the boundary conditions, the electric field is uniquely determined. Accepting this, the rest is straightforward: if we can devise an alternative distribution of (fictitious) charges whose potential satisfies the original Poisson equation and boundary conditions, we have found the solution to the original problem! This fictitious distribution is called the *image charge*. Care is required regarding their placement: they cannot lie within the region where we seek to solve Poisson's equation, otherwise the equation itself would change and we would be solving a different electrostatics problem. Hence, image charges must be placed outside the connected domain in which we wish to find the potential or field. In practice, space is divided into two regions, separated by material interfaces: one where we solve the problem, and one containing all image charges, where the analogous problem is not solved. For example, in the case of a charge outside a conducting sphere, we solve the problem everywhere except inside the sphere, where the images reside. For a charge

near a grounded infinite conducting plane, the problem can be solved only in the half-space containing the real charge; the other half-space contains the image charge that enforces the boundary condition.

What changes in fluid dynamics? For irrotational flows of incompressible inviscid fluids there is an analogue of Poisson's equation. However, the boundary conditions differ: while the electric field at a conductor's surface is normal to it, the velocity near a solid obstacle is tangential to the surface. Water cannot penetrate solids!

Theorem (Analogy). The fluid-dynamic boundary conditions are analogous to the electrostatics ones at the surface of an object described by  $\varepsilon = 0$ .

*Proof.* The interface conditions between two isotropic media are

$$E_{1,\parallel} = E_{2,\parallel}, \qquad \qquad D_{1,\perp} = D_{2,\perp},$$

which imply

$$\varepsilon_1 \tan \alpha_1 = \varepsilon_2 \tan \alpha_2$$

where the angles are measured from the surface normal. If  $\varepsilon_1 = 0$ , then  $\alpha_2 = 0$ . Thus, in medium 2 the field lines are parallel to the surface.<sup>a</sup>

Another difference between the two theories is that, while in electrostatics the value of  $\varepsilon$  determines the orientation of the electric field at a surface, in fluid dynamics there is no analogous parameter that allows different orientations of the velocity at an obstacle's surface. The velocity is always tangential to the surface—there is no alternative. Let us look at some examples.

#### 6.3 Examples of Fields and Flows in 2D

Example 6.1 (Electric field of a charge near a grounded conducting disk). We are in 2D, so the electric field of a point charge is

$$\vec{E}(\vec{r}\,) = \frac{F}{2\pi\varepsilon_0 r}\,\hat{r},$$

with associated potential

$$\varphi_E(r) = -\frac{q}{2\pi\varepsilon_0} \ln r + C.$$

Consider a grounded conducting disk of radius R centered at the origin and a charge q placed along the x-axis at (-d,0) with d > R. Since the field above does not satisfy the boundary condition on the circle, we must place at least one image charge inside the disk. Let us try to place a single image charge  $q_I$  at a distance a < R from the center, as sketched in Fig. 16. The potential generated outside the circle is

$$\varphi_E(r,\theta) = -\frac{q}{2\pi\varepsilon_0} \ln\left(\sqrt{d^2 + r^2 + 2dr\cos\theta}\right) - \frac{q_I}{2\pi\varepsilon_0} \ln\left(\sqrt{a^2 + r^2 + 2ar\cos\theta}\right) + C.$$

We must impose the boundary condition  $\varphi_E(r=R,\theta)=0$ , giving

$$-\frac{q}{2\pi\varepsilon_0}\ln\left(\sqrt{d^2+R^2+2dR\cos\theta}\right)-\frac{q_I}{2\pi\varepsilon_0}\ln\left(\sqrt{a^2+R^2+2aR\cos\theta}\right)+C=0.$$

<sup>&</sup>lt;sup>a</sup>Conversely, if  $\varepsilon_1 \to \infty$ , then  $\alpha_2 \to \pi/2$ . This is what happens for conductors!

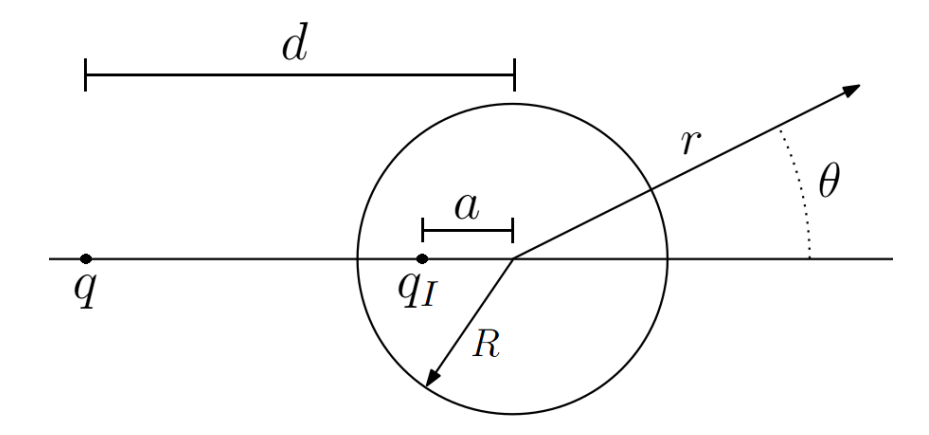


Figure 16: Equivalent configuration with an image charge.

We have one equation but three unknowns. However, it suffices to find a single triplet  $(q_I, a, C)$  that works. The logarithmic terms—the only  $\theta$ -dependent pieces—can be balanced only if  $q_I = -q$ . For the position, let us try with  $a = R^2/d$  as in the 3D sphere case. Then

$$C = -\frac{q}{2\pi\varepsilon_0} \ln \frac{R}{d}.$$

Thus, the potential outside the disk is

$$\varphi_E(r,\theta) = \frac{q}{4\pi\varepsilon_0} \ln \left( \frac{\frac{R^4}{d^2} + r^2 + 2\frac{R^2}{d}r\cos\theta}{d^2 + r^2 + 2dr\cos\theta} \right) - \frac{q}{2\pi\varepsilon_0} \ln \frac{R}{d}.$$

In polar coordinates, the electric field is

$$\vec{E}(r,\theta) = -\nabla \varphi_E = -\frac{\partial \varphi_E}{\partial r} \,\hat{r} - \frac{1}{r} \frac{\partial \varphi_E}{\partial \theta} \,\hat{\theta}. \tag{6.1}$$

Fig. 17 shows the field just outside the conducting disk.

Example 6.2 (Velocity field of a source near a circular obstacle). In 2D, the velocity field of an isotropic source of strength F is

$$\vec{v}(\vec{r}\,) = \frac{F}{2\pi r}\,\hat{r},$$

with associated potential

$$\varphi_V(r) = -\frac{F}{2\pi} \ln \frac{r}{r_0}.$$

Consider a circular obstacle of radius R centered at the origin and a source of strength F on the x-axis at (-d,0) with d > R. Since the field above does not satisfy the boundary condition on the circle, we must place image sources/sinks inside the disk. Why do we know one is not enough? Because the fluid is incompressible: the net fluid produced by the image sources inside the circle must vanish because of the boundary conditions on the velocity. Therefore we need at least a source and a sink of opposite strengths inside. Let their strengths be  $F_I$  and  $-F_I$ , with positions as shown in Fig. 18. This symmetric choice ensures the field is symmetric with respect to the x-axis, and hence vanishes at the circle's intersections with the straight line connecting the three charges.

The potential generated outside the circle is

$$\varphi_V(r,\theta) = -\frac{F}{2\pi} \ln\left(\sqrt{d^2 + r^2 + 2dr\cos\theta}\right) - \frac{F_I}{2\pi} \ln\left(\sqrt{a^2 + r^2 + 2ar\cos\theta}\right) + \frac{F_I}{2\pi} \ln\left(\sqrt{b^2 + r^2 - 2br\cos\theta}\right).$$

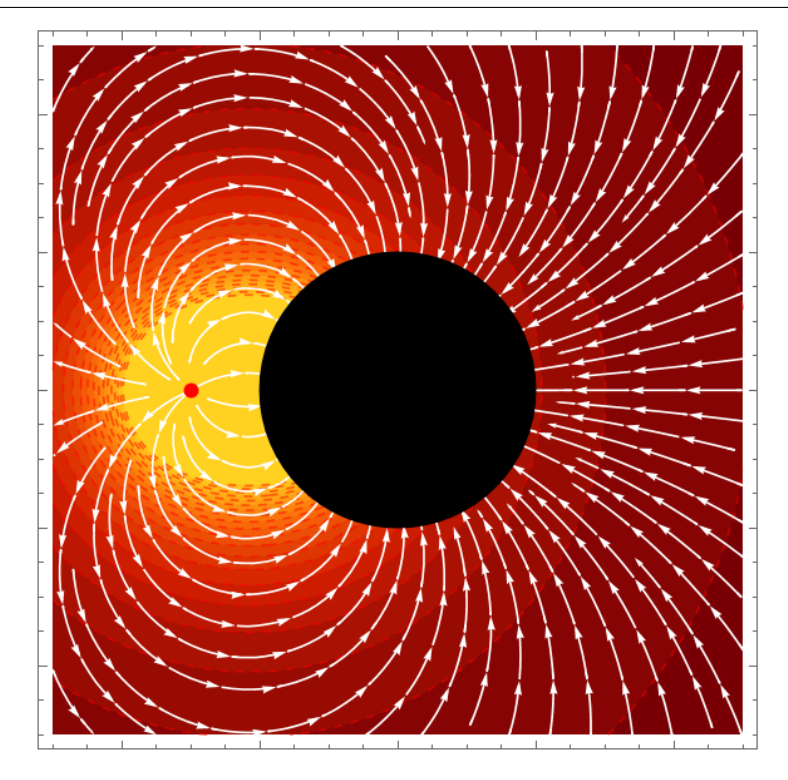


Figure 17: Electric field near the conducting disk for q > 0.

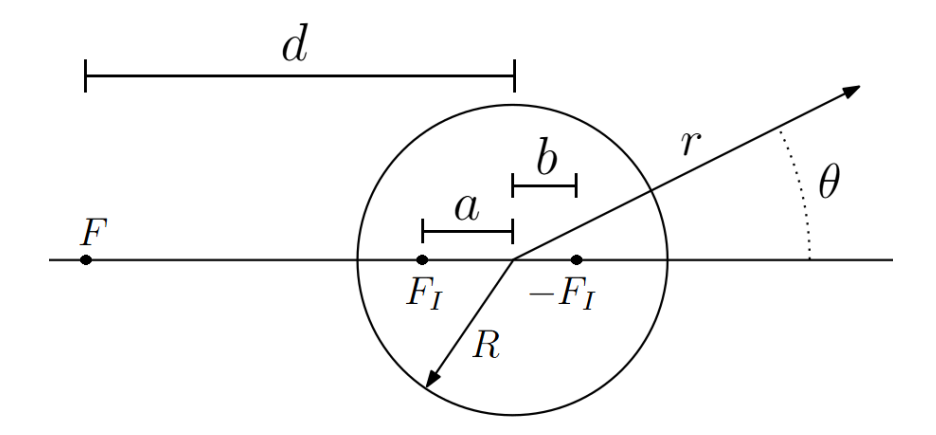


Figure 18: Placement of image sources inside the disk.

In the conducting case the image values/positions enforce constant  $\varphi$  on r = R; here (or in electrostatics with  $\varepsilon = 0$ ) we require the radial component of velocity on the circumference to vanish:

$$v_r \equiv -\frac{\partial \varphi_V}{\partial r} (r = R, \theta) = 0.$$

The radial velocity is

$$v_r(r,\theta) = +\frac{F}{4\pi} \frac{r + d\cos\theta}{d^2 + r^2 + 2dr\cos\theta} + \frac{F_I}{4\pi} \frac{r + a\cos\theta}{a^2 + r^2 + 2ar\cos\theta} + \frac{F_I}{4\pi} \frac{r + a\cos\theta}{b^2 + r^2 - 2br\cos\theta}.$$

Thus the boundary condition becomes

$$\frac{F}{4\pi}\frac{R+d\cos\theta}{d^2+R^2+2dR\cos\theta}+\frac{F_I}{4\pi}\frac{R+a\cos\theta}{a^2+R^2+2aR\cos\theta}-\frac{F_I}{4\pi}\frac{R-b\cos\theta}{b^2+R^2-2bR\cos\theta}=0.$$

This appears to be one equation for three unknowns a, b, and  $F_I$ . However, we only need one working triplet. Let us try guessing b = 0 and  $F_I = F$ . If solving for a yielded a value larger than the radius, the guess would be wrong. The equation reduces to

$$\frac{R+d\cos\theta}{d^2+R^2+2dR\cos\theta}+\frac{R+a\cos\theta}{a^2+R^2+2aR\cos\theta}-\frac{1}{R}=0,$$

whose solution is  $a = R^2/d$ , which is indeed less than R. Hence,  $a = R^2/d$ , b = 0, and  $F_I = F$ . Fig. 19 sketches the setup.

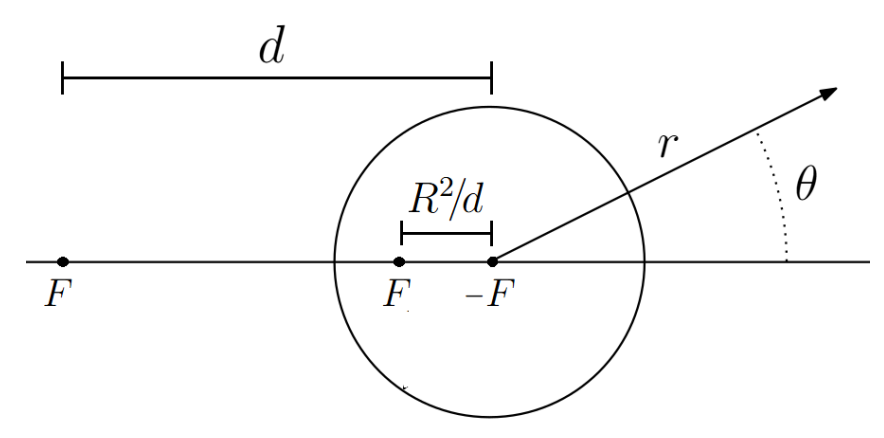


Figure 19: Placement of the image sources inside the disk.

We can now compute the velocity field everywhere. The potential at a generic point becomes

$$\varphi_V(r,\theta) = -\frac{F}{2\pi} \ln\left(\sqrt{d^2 + r^2 + 2dr\cos\theta}\right) - \frac{F}{2\pi} \ln\left(\sqrt{\frac{R^4}{d^2} + r^2 + 2\frac{R^2}{d}r\cos\theta}\right) + \frac{F}{2\pi} \ln r + C.$$

In polar coordinates, the velocity is

$$\vec{v}(r,\theta) = -\nabla \varphi_V = -\frac{\partial \varphi_V}{\partial r} \,\hat{r} - \frac{1}{r} \frac{\partial \varphi_V}{\partial \theta} \,\hat{\theta}. \tag{6.2}$$

Fig. 20 shows the field near the circular obstacle.

**Example 6.3** (River flow around a cylindrical pier). Assuming symmetry along the pier axis, we can treat the configuration as 2D, as in the previous section, with a few tweaks. In the absence of the pier, the river is a uniform, unbounded flow. What configuration of sources produce a uniform field in space? Several constructions work. For instance, an infinite charged plane produces a uniform electric field. Another option is to take two opposite charges +q and -q separated by a distance d and consider the limiting configuration  $q, d \to \infty$  with q/d held constant; the field between them is uniform, like that in a parallel-plate capacitor. Accordingly, let us consider a source +F and a sink -F placed symmetrically at distance d from the center of a cylindrical pier of radius R. We first find the velocity field in this configuration, then take the limit just described. From the previous section, the images at the disk center are equal and opposite and thus cancel. In practice, we only need two image singularities placed as in Fig. 21. The potential in space, excluding the circle, is

$$\varphi_{V}(r,\theta) = -\frac{F}{2\pi} \ln\left(\sqrt{d^{2} + r^{2} + 2dr\cos\theta}\right) - \frac{F}{2\pi} \ln\left(\sqrt{\frac{R^{4}}{d^{2}} + r^{2} + 2\frac{R^{2}}{d}r\cos\theta}\right) + \frac{F}{2\pi} \ln\left(\sqrt{d^{2} + r^{2} - 2dr\cos\theta}\right) + \frac{F}{2\pi} \ln\left(\sqrt{\frac{R^{4}}{d^{2}} + r^{2} - 2\frac{R^{2}}{d}r\cos\theta}\right).$$

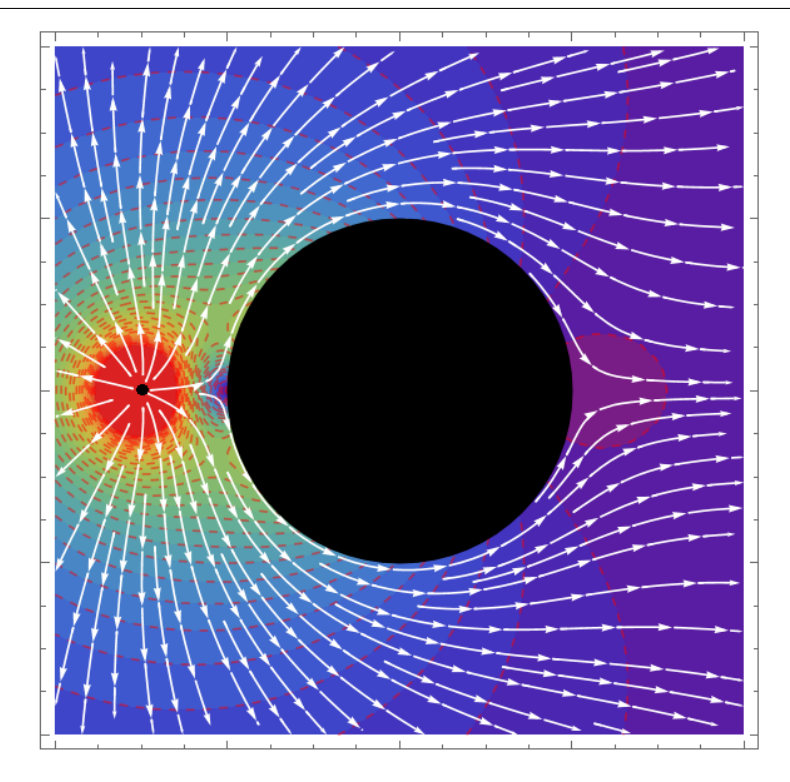


Figure 20: Velocity field generated by a source near a circular obstacle.

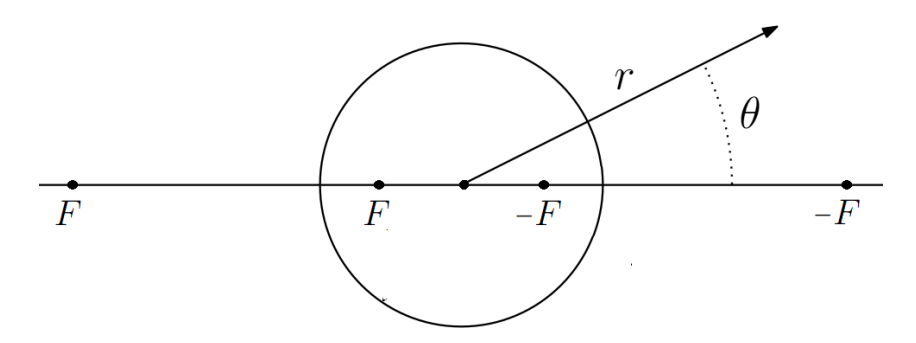


Figure 21: Placement of the real sources and the image sources inside the disk.

Although unnecessary, Eq. (6.2) yields the velocity field in Fig. 22.

We now take the limit  $F, d \to \infty$  with F/d constant. Let us compute it analytically from the potential. Let us expand it in series by factoring d in the first and third terms and r in the second and fourth. Using logarithm properties, the potential reduces to

$$\varphi_{V}(r,\theta) = -\frac{F}{4\pi} \ln\left[1 + \left(\frac{r}{d}\right)^{2} + 2\frac{r}{d}\cos\theta\right] - \frac{F}{4\pi} \ln\left[1 + \frac{R^{4}}{d^{2}r^{2}} + 2\frac{R^{2}}{dr}\cos\theta\right] + \frac{F}{4\pi} \ln\left[1 + \left(\frac{r}{d}\right)^{2} - 2\frac{r}{d}\cos\theta\right] + \frac{F}{4\pi} \ln\left[1 + \frac{R^{4}}{d^{2}r^{2}} - 2\frac{R^{2}}{dr}\cos\theta\right].$$

Since  $d \to \infty$ , each logarithm has the form  $\ln(1+x) \approx x$  with  $x \ll 1$ . Expanding to first order

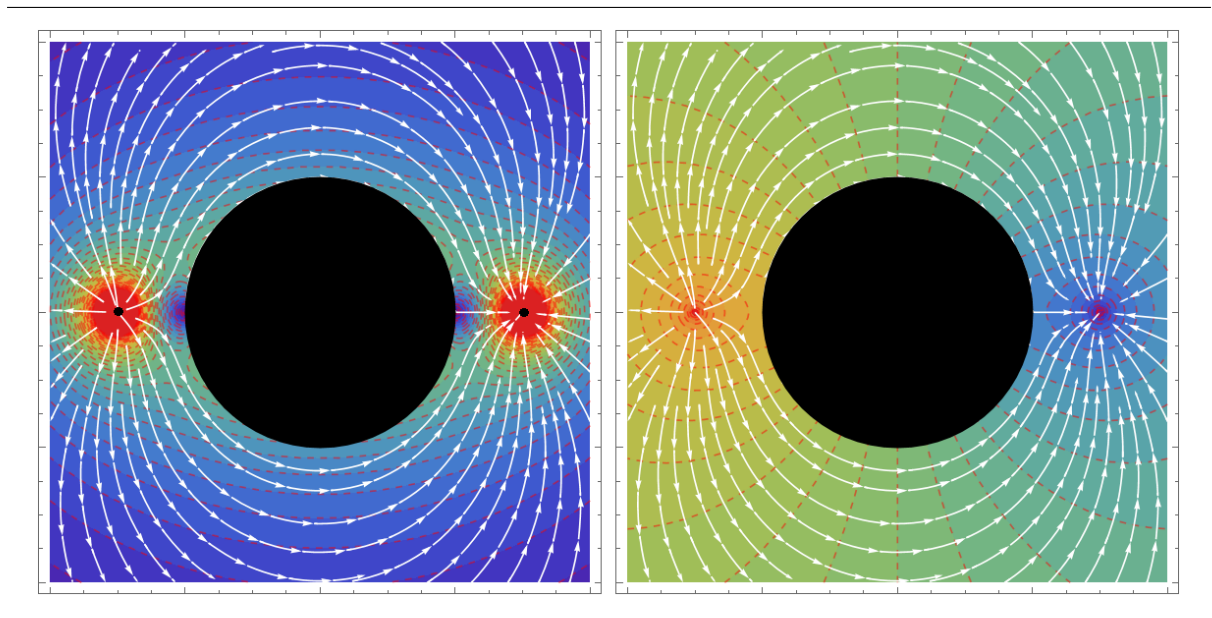


Figure 22: Velocity field generated by a source and a sink near a circular obstacle. Left: magnitude map; right: equipotential lines.

yields

$$\varphi_V(r,\theta) \approx -\frac{F}{4\pi} \left[ \left( \frac{r}{d} \right)^2 + 2\frac{r}{d} \cos \theta \right] - \frac{F}{4\pi} \left[ \frac{R^4}{d^2 r^2} + 2\frac{R^2}{dr} \cos \theta \right] +$$

$$+ \frac{F}{4\pi} \left[ \left( \frac{r}{d} \right)^2 - 2\frac{r}{d} \cos \theta \right] + \frac{F}{4\pi} \left[ \frac{R^4}{d^2 r^2} - 2\frac{R^2}{dr} \cos \theta \right] =$$

$$= -\frac{F}{\pi d} \left( 1 + \frac{R^2}{r^2} \right) r \cos \theta.$$

This implies that the velocity outside the circle is

$$\vec{v}(r,\theta) = -\nabla \varphi_V = \frac{F}{\pi d} \left[ \left( 1 - \frac{R^2}{r^2} \right) \cos \theta \, \hat{r} - \left( 1 + \frac{R^2}{r^2} \right) \sin \theta \, \hat{\theta} \right].$$

For  $\theta = k\pi$  and  $r \to \infty$  (i.e., along the x-axis far from the origin),  $\vec{v} \to F/\pi d \hat{x}$ , so  $F/\pi d$  is precisely the river's current speed, which we may denote by  $U_0$ . We can rewrite

$$\vec{v}(r,\theta) = U_0 \left(\cos\theta \,\hat{r} - \sin\theta \,\hat{\theta}\right) - U_0 \,\frac{R^2}{r^2} \left(\cos\theta \,\hat{r} + \sin\theta \,\hat{\theta}\right),\,$$

where the first term is the uniform background river flow, and the second is the field of a 2D dipole at the origin. This is exactly the field generated by the image singularities, which in this limit sit at the origin because  $d \to \infty$ . The velocity distribution is shown in Fig. 23. The electrostatic analogue is a disk with  $\varepsilon = 0$  immersed in a uniform 2D electric field.

#### 6.4 Examples of Fields and Flows in 3D

Compared to 2D, there are notable differences in 3D. The most evident concerns the values and positions of image charges/sources. For example, for a source near a spherical obstacle, it is no longer sufficient to place two point images as in the 2D disk case. One can show that a point source plus a line distribution of sinks between the sphere's center and the first image position are needed. This difference stems from the different functional form of the 2D and 3D potentials.

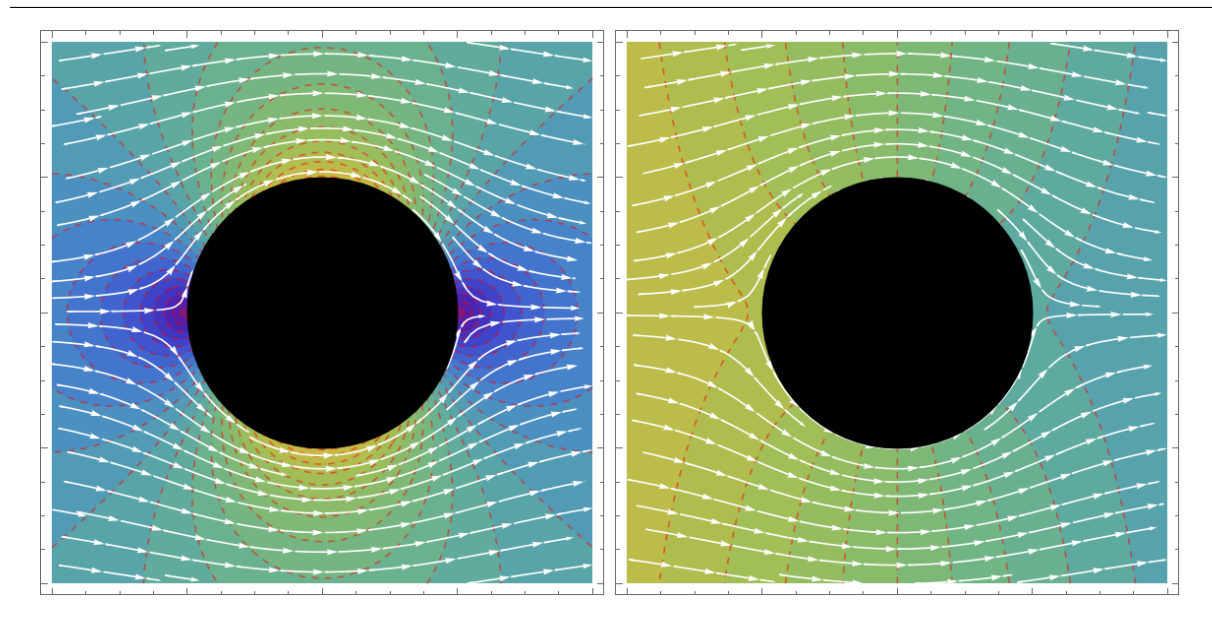


Figure 23: Top view of river flow around a cylindrical obstacle. Left: magnitude map; right: equipotential lines.

In any case, the net flow produced inside the sphere must vanish. For a sphere immersed in a uniform flow, reasoning as for the disk shows that the total field is the sum of the uniform background and the field of a dipole image located within the sphere.

Example 6.4 (Electric field of a charge near a grounded conducting sphere). Consider a grounded conducting sphere of radius R centered at the origin, and a charge q placed along the x-axis at (-d,0) with d > R. We seek an image charge that enforces the boundary condition (field perpendicular to the spherical surface). The potential outside the sphere is

$$\varphi_E(r,\theta) = \frac{q}{4\pi\sqrt{d^2 + r^2 + 2dr\cos\theta}} + \frac{q_I}{4\pi\sqrt{a^2 + r^2 + 2ar\cos\theta}}.$$

Impose

$$\varphi_E(r=R,\theta) = \frac{q}{4\pi\sqrt{d^2 + R^2 + 2dR\cos\theta}} + \frac{q_I}{4\pi\sqrt{a^2 + R^2 + 2aR\cos\theta}} = 0,$$

which is satisfied for  $q_I = -qR/d$  and  $a = R^2/d$ . Therefore,

$$\varphi_E(r,\theta) = \frac{q}{4\pi\sqrt{d^2 + r^2 + 2dr\cos\theta}} - \frac{qR/d}{4\pi\sqrt{\frac{R^4}{d^2} + r^2 + 2\frac{R^2}{d}r\cos\theta}}.$$

The resulting electric field is shown in Fig. 24.

Example 6.5 (Electric field of a charge near a conducting sphere at fixed potential). If the conducting sphere of the previous example is held at a nonzero potential  $V_0 \neq 0$ , it suffices to add another image charge at the center of the sphere of value  $4\pi\varepsilon_0 RV_0$ . Its role is to shift the surface potential from V = 0 (previous example) to  $V_0 \neq 0$ .

Example 6.6 (Electric field of a charge near an infinite conducting plane). Consider a positive charge +q placed at a distance d from an infinite grounded conducting plane. The zero-potential condition on the plane is enforced by an image charge  $q_I = -q$  located at distance d on the opposite side of the plane. The potential in the right half-space is

$$\varphi_E(x,y) = \frac{q}{4\pi\sqrt{(x-d)^2 + y^2 + z^2}} - \frac{q}{4\pi\sqrt{(x+d)^2 + y^2 + z^2}}.$$

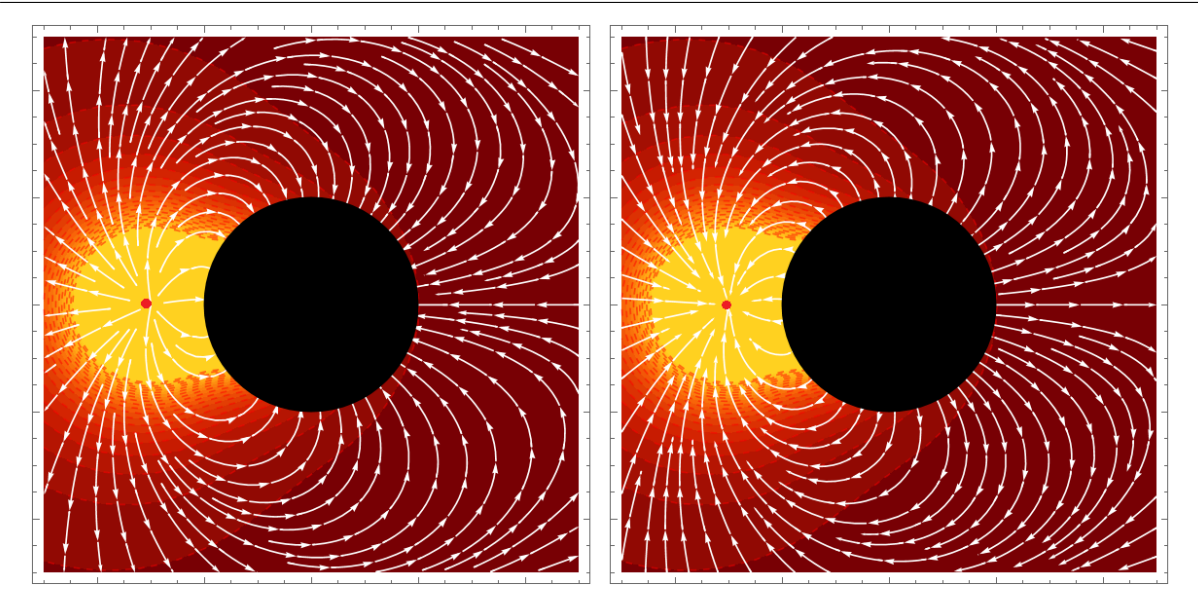


Figure 24: Electric field of a charge (positive on the left, negative on the right) near a grounded conducting sphere.

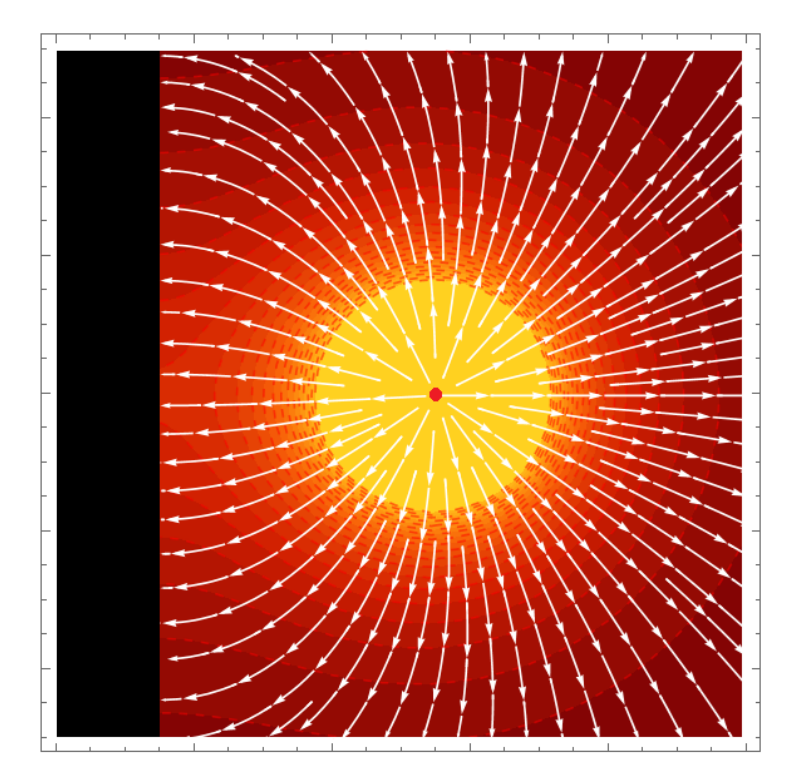


Figure 25: Electric field of a positive charge near an infinite conducting plane.

The resulting field is depicted in Fig. 25.

Example 6.7 (Velocity field of a source near an infinite wall). Consider a source +F placed at a distance d from an infinite wall. The usual tangential-velocity boundary condition is satisfied by placing an image source  $F_I = +F$  on the other side of the wall at distance D, as in Fig. 26. The potential in the right half-space is

$$\varphi_V(x,y) = \frac{F}{4\pi\sqrt{(x-d)^2 + y^2 + z^2}} + \frac{F}{4\pi\sqrt{(x+d)^2 + y^2 + z^2}}.$$

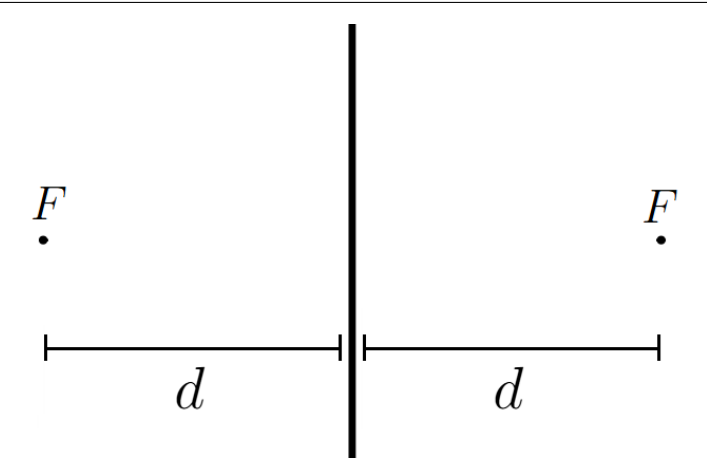


Figure 26: Source (right) and image source (left).

Computing the velocity yields the distribution in Fig. 27.

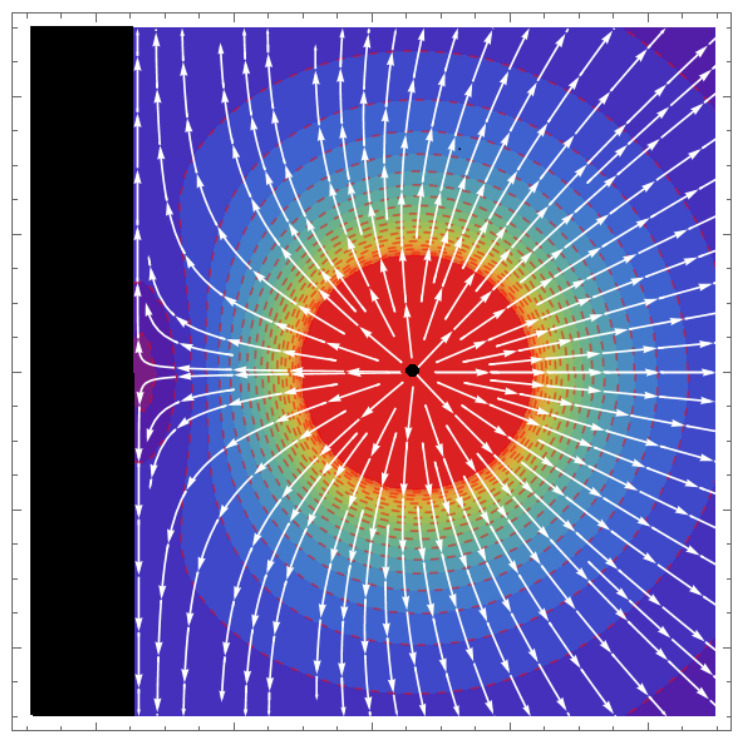


Figure 27: Velocity field generated by a source near a wall.

#### 6.5 Force on Conductors and Obstacles

In all electrostatic configurations considered so far, a force arises between the conductor and the external fixed charge. This force is always attractive, regardless of the charge's sign. One may compute it by first finding the induced surface-charge density on the conductor (via Coulomb's theorem) and then integrating all the tiny contributions; the result matches the force obtained from the interaction between the real charge and the image charges.

In fluid dynamics the situation is different: under our assumptions (steady, irrotational, incompressible, inviscid flow with ordered streamlines), the reduced Bernoulli's theorem holds: the quantity

$$B = p(\vec{r}) + \frac{1}{2}\rho v^2(\vec{r})$$

is the same at every point in the fluid, except at sources and sinks. $^{12}$  The force on an obstacle is thus

$$\vec{F} = \int_{S} p(\vec{r}) \,\hat{n} \, dS = \int_{S} B \,\hat{n} \, dS - \frac{1}{2} \rho \int_{S} v^{2}(\vec{r}) \,\hat{n} \, dS, \tag{6.3}$$

with the integral taken over the obstacle surface. Consider two special cases:

- 1. For finite obstacles, the first term vanishes because the integral of the inward normals over a closed surface is zero.
- 2. For finite obstacles in sufficiently symmetric flows, the second integral vanishes. This occurs, for example, for an object in a uniform flow. This counterintuitive result is known as d'Alembert's paradox.

Accordingly, the force on the disk in Fig. 20 is nonzero and directed toward the source, contrary to naive expectation. Indeed, the last term in Eq. (6.3) "pulls" to the left because  $v^2(R,\theta)$  is larger on the left hemisphere. In the configurations of Fig. 22 and Fig. 23 the force vanishes because  $v^2(R,\theta) = v^2(R,-\theta)$ , whereas the force on the wall in Fig. 27 tends to push it leftward, regardless of whether there is a source or a sink.

 $<sup>^{-12}</sup>$ At sources/sinks the incompressibility assumption fails. Moreover, near these points the velocity is formally unbounded, which might suggest negative pressures to keep B constant. In reality, pressure cannot be negative, so a different interpretation is required: when sources/sinks are present (with divergent local velocities), the value of B is effectively infinite, which coincides with the pressure at infinity, where the velocity vanishes. This is merely a formal device to keep everything consistent.